analytical chemistry

Review

pubs.acs.org/ac

Recent Advances in Electrochemical Immunosensors

Wei Wen,[†,§] Xu Yan,[†,§] Chengzhou Zhu,[†] Dan Du,[*,†,‡] and Yuehe Lin[*,†]

[†]School of Mechanical and Material Engineering, Washington State University, Pullman, Washington 99164, United States

[‡]Key Laboratory of Pesticide and Chemical Biology of Ministry of Education, College of Chemistry, Central China Normal University, Wuhan, Hubei 430079, P.R. China

CONTENTS

Due to the combination of specific antigen−antibody recognition with the high sensitivity of electrochemical methods, electrochemical immunosensors (EIs) have aroused considerable interest, and significant progress has been achieved in the early diagnosis and clinical analysis of disease states, food safety control, environmental monitoring, public security, home-health care, etc. In recent decades, EIs have exhibited many intrinsic advantages, including remarkable sensitivity, operational simplicity, low-cost instrumentation, inherent miniaturization, and potential of automation, and have provided elegant routes for the detection of trace amounts of analytical targets of biological significance ranging from small molecules (e.g., haptens and natural toxins) and macromolecules (e.g., antigens and disease biomarkers) to cells, pathogenic bacteria, or viruses.[1] Various electrochemical methodologies, such as voltammetry and amperometry, electrochemiluminescence, photoelectrochemistry, impedance, potentiometry, piezoelectricity, field-effect transistor, and alternating current electrohydrodynamics, have been employed in the development of immunoassays to achieve high sensitivity in terms of the electrochemical change of signal transduction. Moreover, electrode arrays and chips have been developed for the simultaneous multiplex high-throughput analysis of complex samples. In particular, numerous attempts have been made to construct hand-held devices with inexpensive 3D-printed converters, integrated microfluidic systems, and paper-based platforms, and substantial improvements have been made to analytical processes and promising applications for point-of-care (POC) diagnostics.[2]

This Review focuses on the recent development of EIs from past two years, with a particular emphasis on the conventional electrochemical methodologies of voltammetry and amperometry, electrochemiluminescence, photoelectrochemistry and impedance, and emerging devices and electroanalytical platforms (Figure 1). Rather than focusing on a comprehensive coverage of all developments in EIs as has been performed in other general reviews,[3,4] we attempted to provide readers with a panoramic snapshot of the most exciting and high-impact recent advances that have been made in this dynamically developing field from our point of view. Nanomaterial-enhanced signal amplification, enzyme-based signal amplification, and DNA facilitating amplified detection have been used more frequently in EIs to achieve high sensitivity in the past two years and have exhibited great superiority.[5] New advances in the utilization of novel types of redox-active species, the application of nanobodies (NBs) as biorecognition elements, immunosensor fabrication using more efficient blocking reagents or through the oriented immobilization of antibodies, and novel devices and platforms that are used in the integration and automation of EIs are reviewed herein.[6] Beyond a discussion of the recent demonstrations of new detection devices and emerging techniques, we also offer a commentary and perspectives regarding EIs, as well as how future advances might impact the commercialization opportunities and POC

Special Issue: Fundamental and Applied Reviews in Analytical Chemistry 2017

Published: November 9, 2016

DOI: 10.1021/acs.analchem.6b04281
Anal. Chem. 2017, 89, 138−156

Figure 1. Schematic illustration for various EIs and their bioanalytical applications. Reproduced from Yang, Z.; Zhuo, Y.; Yuan, R.; Chai, Y. *Anal. Chem.* **2016**, *88*, 5189−5196 (ref 53). Copyright 2016 American Chemical Society. Reprinted from Wang, J.; Zhuo, Y.; Zhou, Y.; Wang, H.; Yuan, R.; Chai, Y. *ACS Appl. Mater. Interfaces* **2016**, *8*, 12968−12975 (ref 71). Copyright 2016 American Chemical Society. Reproduced from Fan, G. C.; Zhu, H.; Du, D.; Zhang, J. R.; Zhu, J. J.; Lin, Y. *Anal. Chem.* **2016**, *88*, 3392−3399 (ref 102). Copyright 2016 American Chemical Society. Reproduced from Zhu, Y. C.; Zhang, N.; Ruan, Y. F.; Zhao, W. W.; Xu, J. J.; Chen, H. Y. *Anal. Chem.* **2016**, *88*, 5626−5630 (ref 106). Copyright 2016 American Chemical Society. Reprinted from *Biosens. Bioelectron.*, Vol. *84*, Chuang, C. H.; Du, Y. C.; Wu, T. F.; Chen, C. H.; Lee, D. H.; Chen, S. M.; Huang, T. C.; Wu, H. P.; Shaikh, M. O. Immunosensor for the ultrasensitive and quantitative detection of bladder cancer in point of care testing, pp. 126−132 (ref 120), Copyright 2016, with permission from Elsevier. Reproduced from Aroonyadet, N.; Wang, X.; Song, Y.; Chen, H.; Cote, R. J.; Thompson, M. E.; Datar, R. H.; Zhou, C. *Nano Lett.* **2015**, *15*, 1943−1951 (ref 149). Copyright 2015 American Chemical Society. Reprinted from *Biosens. Bioelectron.*, Vol. *71*, Li, S.; Wang, Y.; Ge, S.; Yu, J.; Yan, M. Self-powered competitive immunosensor driven by biofuel cell based on hollow-channel paper analytical devices, pp. 18−24 (ref 173), Copyright 2015, with permission from Elsevier. Reprinted from *Biosens. Bioelectron.*, Vol. *86*, Aronoff-Spencer, E.; Venkatesh, A. G.; Sun, A.; Brickner, H.; Looney, D.; Hall, D. A. Detection of Hepatitis C core antibody by dual-affinity yeast chimera and smartphone-based electrochemical sensing, pp. 690−696 (ref 232), Copyright 2016, with permission from Elsevier.

diagnostics. Because of the explosion of scholarly articles that are relevant to this extremely broad field of research, we have undoubtedly missed many important contributions during the above referenced time period, and we sincerely apologize to the authors for their important work that may have been overlooked.

IMMUNOSENSORS BASED ON VOLTAMMETRY AND AMPEROMETRY

Regarded as a subset of EIs, voltammetry and amperometry is the most popular and the most common electrochemical method that is used to probe various immunoreactions due to its wide applicability and high sensitivity.[7] The highly sensitive determination of various biochemical species is of great significance for the elaboration of the behavior of life, the early diagnosis and prevention of disease, and the screening and development of new drugs.[8] Signal amplification is a core competence of the design of manifold high-performance immunosensing protocols for targets that are present in low abundance. In the past two years, signal-amplified detection in EIs was accomplished via three general strategies: nanomaterial-enhanced, enzyme-based, and DNA-based signal amplification.

Nanomaterial-Enhanced Amplification. Nanomaterials have numerous remarkable properties that can improve the sensitivity of EIs through various amplification mechanisms. (1) Nanomaterials have large surface areas and extraordinary electron-transfer abilities. When conjugated to proteins (antigen or antibodies) with insulating features or when immobilized on a solid electrode, nanomaterials can increase the effective surface area of modified electrodes and can also accelerate the electron-transfer rate of electroactive species.[9,10] (2) Nanomaterials exhibit a fascinating catalytic activity and are widely utilized as state-of-the-art electrocatalysts to enlarge responding electrochemical signals. Our group recently offered comprehensive reviews of graphene and graphene-like nanomaterial-based biosensing applications.[11,12] (3) Due to their favorable biocompatibility and multivalent affinity interactions with proteins through electrostatic, hydrophobic, or $\pi-\pi$ stacking interactions, nanomaterials are usually exploited as nanocarriers for receptor molecules and are multilabeled with a high molar ratio of enzyme to antibody for amplified immunoreactions.[11] (4) With the built-in amplification feature, nanomaterials can be employed as biolabels or as redox nanoprobes. For example, nanoparticles of metals and their compounds are often used as nanobiomarker probes since each nanoparticle contains thousands of metal atoms that can be detected via anodic stripping voltammetry with significant signal amplification.[13]

Singh and Krishnan[14] prepared a conductive multiwall carbon nanotube (MWCNT)-pyrenebutyric acid framework on graphite electrodes for the detection of serum insulin with a detection limit of 15 pM. As a typical example, the functionalization of carbon nanotubes with pyrenebutyric acid provided a large specific surface area for high-density immobilization of anti-insulin antibodies and displayed a significant improvement in biological signal transmission. Our group[15] developed a dual enhancing strategy for the ultrasensitive detection of α-fetoprotein (AFP) by a polydopamine functionalized N-doped MWCNT (PDA-N-MWCNT) and the composite of graphene loaded mesoporous Au@Pt nanodendrites. The PDA-N-MWCNT nanocomposites not only provided an exceptional biocompatible surface with a larger electroactive area on which to immobilize antibodies but also enhanced the electron-transfer rate to drastically improve the sensitivity of the amperometric immunosensor. Novel nanomaterials, such as wire-in-tube iridium oxide,[16] mesoporous zinc oxide nanofibers,[17] ultralong CuS nanowires,[18] and shape-controlled gold nanoparticle (AuNP) decorated thionine−MoS_2 nanocomposites,[19] were synthesized and deposited on various electrodes to accelerate electron-transfer kinetics. Recently, Wei and co-workers described a series of nanomatrixes, $CoFe_2O_4$/graphene nanohybrids,[20] carbon encapsulated Fe_3O_4 magnetic nanocomposites,[21] and multifunctional magnetic graphene nanocomposites,[22] which were used as supports of an EI to increase the loading capacities of various antibodies and to enlarge the responding signal of the immunosensor.

In addition to their function as electrode materials, nanomaterials, especially metal and metal oxide nanomaterials, have been extensively harnessed as catalytic reagents in numerous electrochemical reactions. With properties that are similar to a natural peroxidase, Pt, MnO_2, and Fe_3O_4 nanoparticles exhibit excellent electrocatalytic ability toward H_2O_2. A nonenzymatic EI that used Fe_3O_4@MnO_2@Pt nanocomposites as multiple signal amplifiers was found to

DOI: 10.1021/acs.analchem.6b04281
Anal. Chem. 2017, 89, 138−156

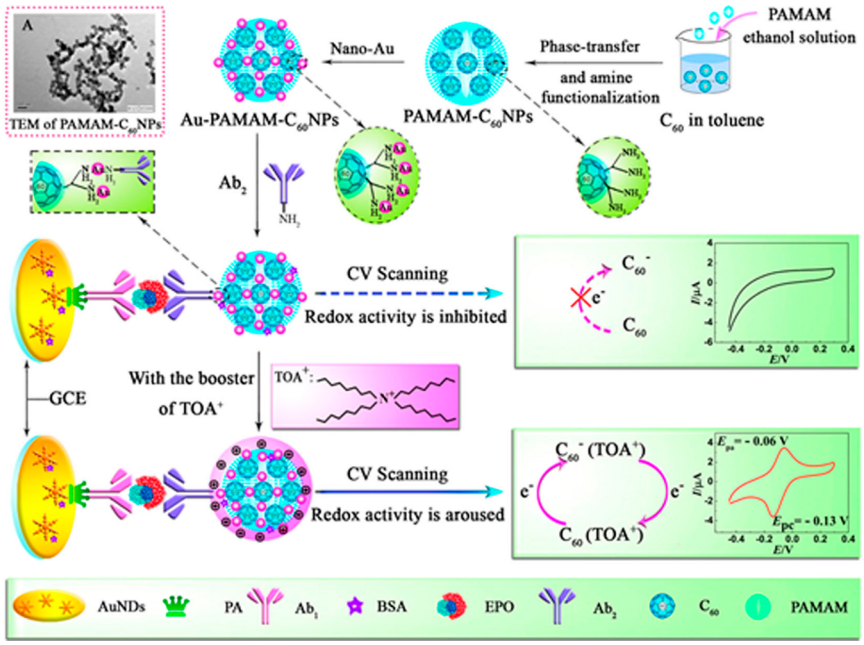

Figure 2. Schematic diagram of the immunosensor preparation process and the possible mechanism of an electrochemical reaction with C_{60}-based nanomaterials as redox nanoprobes. Reproduced from Han, J.; Zhuo, Y.; Chai, Y. Q.; Xiang, Y.; Yuan, R. *Anal. Chem.* **2015**, *87*, 1669−1675 (ref 37). Copyright 2015 American Chemical Society.

sensitively detect carcinoembryonic antigen (CEA).[23] There are several advantages of Fe_3O_4@MnO_2@Pt nanocomposites. First, Fe_3O_4 nanoparticles facilitate magnetic separation. Furthermore, the thin-layer MnO_2 nanosheets offer a large surface area for the catalysis of H_2O_2 and can also closely interact with Fe_3O_4 and Pt nanoparticles. The Fe_3O_4@MnO_2@Pt nanocomposites produce a synergistic effect that enhances the catalytic reduction of H_2O_2. The immunosensor exhibits a high sensitivity and acceptable selectivity for CEA, with a dynamic working range from 0.5 pg mL^{-1} to 20 ng mL^{-1} and a detection limit of 0.16 pg mL^{-1}. A gold nanocatalyst was also prepared to develop an ultrasensitive and incubation-free EI that used outer-sphere to inner-sphere electrochemical-nanocatalytic redox cycling for high signal amplification.[24] As the size, shape, and surface properties affect the catalytic activity of AuNPs, poly(amidoamine) (PAMAM) was utilized as a template to prevent AuNP aggregation and to precisely control the nanosize. PAMAM-Au has been applied in the construction of an enzyme-free EI for procalcitonin detection.[25] The PAMAM-Au acts not only as a nanocatalyst to catalyze the oxidation of ascorbic acid but also as a nanocarrier to anchor large amounts of antibodies for signal amplification. As such, due to their excellent catalytic activities, mesoporous carbon-enriched palladium nanostructures,[26] zinc oxide 1D nanorods and 2D nanoflakes,[27] and silver nanocluster/graphene oxide nanocomposites[28] are typically used as candidates in amperometric immunoassays.

Another important application of nanomaterials in electrochemical immunoassays is the utilization of nanomaterials as nanocarriers for antibodies and enzymes or other labels. With the excellent suspension in aqueous solution, a high chemical stability, and an abundance of reactive silanol on the surface for bioconjugation, the use of silicon nanoparticles as antibody and enzyme nanohost provides an effective way to implement a signal amplification strategy. Tang and co-workers[29] reported an enzymatic hydrolysate-triggered displacement reactive strategy for the detection of aflatoxin B_1 (AFB_1) using silica nanoparticles that were doped with a horseradish peroxidase (HRP)-thionine conjugate as the trace tag. After the covalent conjugation of a monoclonal anti-AFB_1 antibody and concanavalin A, the multifunction silica nanoparticles were immobilized on a dextran-modified sensing interface to construct an immunosensor. The ultrasensitive immunosensor demonstrated a linear range from 3.0 pg mL^{-1} to 20 ng mL^{-1}, with a detection limit of 2.7 pg mL^{-1}. As a new type of functionalized unit for the fabrication of an EI to date, Mo_2C nanomaterials were explored as nanocarriers to load thionine molecules through $\pi-\pi$ and electrostatic interactions for AFP detection.[30] Trimetallic NiAuPt nanocomposites[31] and gold nanorods with different aspect ratios[32] were also employed to enhance the attachment amount of biomolecules and to improve the electrochemical responses of immunosensors.

In addition to the above applications, the use of metal nanomaterials and their compounds themselves as redox probes has been shown to be a promising approach to amplify the response of the immunoassay. Xie and co-workers[33] described a sandwich immunoassay method that used AuNPs for the duple amplification of biolabel signals. The method can be sensitive to a few antigen molecules and is based on gold-stained AuNPs through the redox reaction of $HAuCl_4$−NH_2OH to enlarge the size of AuNPs and on in situ anodic stripping voltammetry detection with the cathodic preconcentration of the second antibody labeled AuNPs. PdPt nanocages, with hollow interiors and porous walls, were used as nanolabels in EIs for the detection of CEA because of their efficient catalytic activity toward H_2O_2 reduction.[34] Multiplexing detection could be used to enhance the accuracy of the diagnosis of critical diseases in humans in the early stages and is one of the major challenges in the generation of EIs. The elaborate utilization of multiple redox probes with electrochemical activity is a key issue for the simultaneous detection of multiple targets. To circumvent this issue, Ma and co-workers[35] synthesized three types of redox-

DOI: 10.1021/acs.analchem.6b04281
Anal. Chem. 2017, 89, 138−156

active species for the voltammetric detection of multiple biomarkers of lung cancer. Gold-poly(*o*-aminophenol), gold-poly(*o*-phenylenediamine), and gold-poly(*p*-phenylenediamine), which can produce oxidation peaks at −0.2, −0.5, and 0.25 V, respectively, were successfully used as signal tags. Special attention should be paid to some emerging nonmetallic nanomaterials as redox probes. Our group[36] also reported a simultaneous electrochemical immunoassay of phosphorylated proteins that used different apoferritin template metallic phosphates as distinguishable signal reporters. Very recently, C_{60}-based nanomaterials were adequately utilized as a new type of redox nanoprobe in EIs for doping detection.[37] In this work, as shown in Figure 2, C_{60} nanoparticles were prepared and functionalized with polyamidoamine and AuNPs. Under the assistance of surfactant tetraoctylammonium bromide as a booster to raise the inner redox activity of the C_{60}-based nanomaterials, a pair of reversible redox peaks was observed. This proposal paves a novel avenue for the exploration of carbon nanomaterials as redox nanoprobes in the electrochemical immunoassay field.

Enzyme-Based Amplification. Enzyme-based amplification immunoassays take advantage of fast and selective catalytic enzyme reactions and are the most common high-efficiency methods in the EI field because a single enzyme molecule, for instance, HRP, can generate 10^7 molecules of product per minute.[29] HRP,[38−40] alkaline phosphatase (ALP),[41,42] and glucose oxidase (GOx)[43−45] are usually exploited as potential candidates for enzyme labels. Yin's group[46] fabricated an EI for 5-hydroxymethylcytosine (5-hmC) detection using avidin-functionalized ALP as a label. In many cases, enzymatic amplification can be combined with other signal amplification strategies, such as chemical−chemical (CC) redox cycling, to obtain higher signal amplification. During redox cycling, the enzyme product can regenerate from a preexisting agent (a reducing or oxidizing agent) in the solution, which results in the sensitive detection of analytes. Inspired by the above method, an ALP enzymatic Ag-deposition protocol with CC redox cycling was reported by Yang's group[47] for the detection of creatine kinase-MB. On the basis of a similar scheme, Akanda and Ju[48] reported a tyrosinase (Tyr)-responsive electrochemical−chemical (EC) redox cycle for the immunodetection of CEA with a high sensitivity and a wide dynamic range. In the detection system that was designed, the Tyr, as an immunoassay label, can convert a weakly electroactive phenol to a highly electroactive catechol to trigger a β-nicotinamide adenine dinucleotide disodium salt (NADH)-related catalysis, which leads to a high signal-to-noise ratio for the immunoassay. To minimize electrochemical signal interference, Yang and coworkers designed a washing-free EI with glycerol-3-phosphate dehydrogenase (GPDH) as an enzyme label. Because the reaction of GPDH with dissolved O_2 is low and the electrochemical interference of $Ru(NH_3)_6^{2+}$, an electrochemical oxidation product generated by GPDH, is also very low, the immunosensing scheme can be applied to detect cardiac troponin I in human serum with low interference and without washing. The washing-free and low-interference EIs show invaluable promise for applications in the disposable and miniaturized immunosensing field.[49]

DNA-Based Amplification. DNA-based amplification contributes to the electrochemical immunoassay field via the introduction of current DNA nanotechnology signal amplified strategies such as hybridization chain reaction (HCR), nuclease-assisted target recycling, rolling circle amplification (RCA), etc., for highly sensitive protein detection.[50,51] Typically, by utilizing a DNA labeled antibody, the specific recognition event of an antibody to a target antigen can be augmented by the conversion of the immunoreaction into an output of single-stranded DNA via proximity hybridization and DNA strand displacement. This reaction can trigger an amplification process to generate more of the signal reporters or their surrogates by using numerous DNA nanotechnology strategies. For example, Ju and co-workers[52] described a target-triggered triple-binder assembly of MNAzyme for a signal amplified immunoassay of CEA. Using three DNA-conjugated antibodies, the target protein drove the proximity hybridization of DNA to produce the Mg^{2+}-dependent MNAzyme, which autocatalytically cleaved the methylene-blue labeled hairpin DNA on the electrode surface to depress the electrochemical oxidation signal of methylene blue. The immunoassay method demonstrated a high sensitivity toward CEA with a detection limit of 1.5 pg mL^{-1}. Yuan's group[53] described a protein conversion strategy for the electrochemical immunoassay of cystatin C using immunoreaction-driven DNA strand displacement and exonuclease-assisted target cyclic signal amplification. Combined with an HCR signal amplification protocol, the immunosensor exhibited a wide dynamic working range from 0.01 pg mL^{-1} to 30 ng mL^{-1} with a detection limit of 3 fg mL^{-1}. DNA concatemer, a linear polymeric structure that is produced via HCR or through a hybridization reaction of short DNA fragments, was also employed for the amplification of signal detection. After different signal molecules are selected to label short DNA fragments, numerous signal molecules can attach to the long DNA concatemer to amplify the electrochemical signal. Zhang and co-workers[54] described a multiplexed immunoassay for AFP and prostate specific antigen (PSA) that was based on a DNA HCR amplification signal. Hemin/G-quadruplex concatemer electrocatalytic amplification[55] and isothermal cycling signal amplification[56] strategies were also successfully investigated in EIs for the amplified detection of diverse biomolecules.

Other Approaches. Some novel electrochemical detection strategies and technologies have been skillfully exploited in EIs during this two year period. NBs, which are variable domains of heavy-chain antibodies, have been utilized in immunoassays as specific biorecognition elements. An NB-based stripping voltammetric immunosensor was exploited by Wan and coworkers for the detection of apolipoprotein-A1 (Apo-A1) using silver nanoparticles as probes.[57] In this scheme, NB (NB11 and NB19), which can bind to different epitopes of Apo-A1, is a distinct type of antibody fragment that is obtained from the serum of camelids. Very recently, Wan and co-workers[58] also reported a highly sensitive and selective immunoassay of Cry1C using NB and graphene oxide/thionine assembly by square wave voltammetry. Compared with conventional monoclonal antibodies, NB exhibits smaller sizes, lower steric hindrance, higher binding specificity, and good thermal and chemical stability. In light of the fact that the application of NB in EIs is still limited, research on NB and its promising application in clinical examination should be addressed in the future.

The development of a rational and highly efficient sensing interface that can selectively recognize a target and depress the nonspecific adsorption of contaminants is of vital importance for an EI. Smaller blocking species in an EI can exhibit lower steric hindrance effects without hindering a specific immune reaction between an analyte and its antibody. Inspired by this protocol, Lin's group[59] investigated an inactive small peptide,

DOI: 10.1021/acs.analchem.6b04281
Anal. Chem. 2017, 89, 138−156

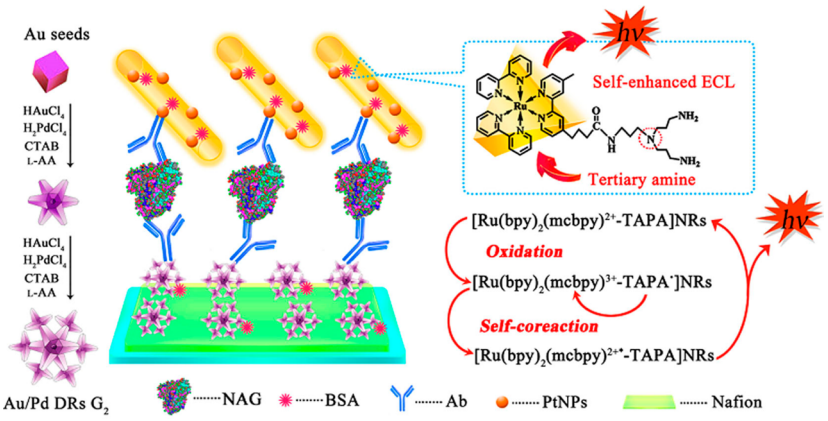

Figure 3. Fabrication of the immunosensor and the reaction mechanism. Reproduced from Wang, H.; Yuan, Y.; Zhuo, Y.; Chai, Y.; Yuan, R. *Anal. Chem.* **2016**, *88*, 2258−2265 (ref 70). Copyright 2016 American Chemical Society.

oxidized glutathione (GSSG), as a replacement for a conventional blocking reagent, bovine serum albumin (BSA), for the fabrication of an immunosensor. The GSSG-blocking-based EI reached a very low detection limit of 0.01 pM for the detection of epidermal growth factor, which was more sensitive than the BSA blocking strategy. This protocol established a new blocking strategy in an immunoassay for the detection of disease-related species at an extremely low concentration.

IMMUNOSENSORS BASED ON ELECTROCHEMILUMINESCENCE

The electrochemiluminescence (ECL) immunosensor as a sensitive detection platform has attracted significant interest due to its advantages of low background and high selectivity.[60] The ECL immunosensor combines the high specificity of antibody recognition elements with the sensitivity of signal transduction and amplification technology. Thus, signal amplification approaches become essential in the development of a highly sensitive immunosensor. Muzyka[61] reviewed the development of ECL-based immunosensors in terms of new formats, labels, and immobilization support. The following are recent achievements in signal amplification strategies that have focused on the development of nanomaterial-enhanced amplification and DNA hybridization amplification.

Nanomaterial-Enhanced Amplification. Owing to remarkable achievements in material science, a novel functional nanomaterial-based electrochemical signal amplification strategy has emerged as a promising candidate for the improvement of both sensitivity and selectivity of ECL-based immunosensors. Most of the biosensors that are discussed below employ new electrode materials and novel functional nanomaterials. Electrode materials have served as significant parts in high-performance ECL immunosensors. Advanced electrode materials may not only improve the electrical conductivity but also increase the surface area, both of which can enhance the sensitivity of an ECL immunosensor. Habtamu et al.[62] described a novel ECL immunosensor for the diagnosis of celiac disease by using membrane-templated gold nanoelectrode ensembles (NEEs) with remarkable properties. This sensing platform was based on the physical segregation between the initial electron-transfer reactions at gold nanodisks and the location of the ECL-emitting region. When NEEs were embedded in a polymeric template, numerous reactive radicals were generated that could efficiently produce the electrochemical signal, which enhanced the ECL signal. The proposed assay showed a good linearity in the range from 1.5 ng mL^{-1} to 10 μg mL^{-1}.

Pang et al.[63] presented a label-free ECL immunoassay for the high-sensitivity analysis of CEA. Due to their large specific surface area and superior conductivity, graphene oxide/carboxylated multiwall carbon nanotubes (GO/MWCNTs-COOH) were used to load gold, cerium oxide nanoparticles (CeO_2), and antibodies. CeO_2 nanoparticles and $K_2S_2O_8$ were exploited as a luminescent material and a coreactant, respectively. The strategy was excellent for CEA detection and exhibited a low detection limit (0.02 ng mL^{-1}). Many other nanomaterials have been grafted onto an electrode surface for the fabrication of ECL immunosensors, such as *N*-(aminobutyl)-*N*-(ethylisoluminol) functionalized gold dots/chitosan/MWCNTs,[64] poly(ethylenimine)/Ru(bpy)$_3^{2+}$-doped silica nanoparticle complexes,[65] AuNPs modified reduced graphene oxide (rGO),[66] Pb-β-cyclodextrin/silver nanoparticle hybrid materials,[67] and Au/Ag-rGO/graphene quantum dots (QDs).[68] These fabricated electrodes improved the performances of ECL sensors.

Functional nanomaterials, which directly linked to an antibody, can also amplify biorecognition events and can be used to create a highly sensitive ECL immunosensor. Zhang et al.[69] designed a spectral ECL immunoassay for the highly sensitive detection of AFP by using a homemade spectral acquiring system. In this sandwich-type immunosensor format, due to its high stability and passivated surface states, ternary CdZnSe nanocrystals that served as antibody tags could be repeatedly injected with electrons, which resulted in a strong cathodic ECL signal and amplified the electrochemical signal. The spectral-based ECL immunosensor showed a linear relationship from 0.10 to 50.0 pg mL^{-1} for AFP, as well as a low detection limit of 0.010 pg mL^{-1}.

Wang et al.[70] developed a self-enhanced ECL immunosensor for the sensitive detection of *N*-acetyl-β-D-glucosaminidase (NAG). The authors successfully synthesized ruthenium(II)-based nanorods through a solvent evaporation-induced self-assembly procedure by using bis(2,2′-bipyridyl) (4′-methyl-[2,2′] bipyridinyl-4-carboxylicacid) ruthenium(II)/tris(3-aminopropyl)amine composite (Figure 3). Due to the combination of luminescent material and a coreactant chemical to form nanorods, the intramolecular reaction shortened the electron-transfer path and lessened energy loss, which could highly improve luminous efficiency and thus enhance signal amplification. Moreover, the nanorods with a large surface area

DOI: 10.1021/acs.analchem.6b04281
Anal. Chem. 2017, 89, 138−156

can efficiently absorb Pt nanoparticles to enhance the electrical conductivity. On the basis of sandwiched immunoreactions, the proposed platform showed excellent linearity at 0.5 pg mL^{-1} to 1 ng mL^{-1}. In another work, Wang et al.[71] utilized ceria doped ZnO nanomaterials to load the antibody and luminol as a signal probe, which can generate a strong ECL signal. Then, the H_2O_2 enzymatic reaction was further catalyzed to produce reactive oxygen species, which promoted the signal of the ECL immunosensor.

Many new carriers were prepared to improve the loading of the antibody, which could enhance the sensitivity of an immunosensor.[72,73] For example, Zhou et al.[74] developed a novel and sensitive ECL immunosensor for human immunodeficiency virus type 1 (HIV-1) p24 antigen determination by incorporating the amplification of AuNP-decorated graphene. The resultant nanocomposite exhibited a large specific surface area as a nanocarrier on which to load multiantibody and $Ru(bpy)_3^{2+}$-doped silica nanoparticles. Moreover, the resultant functionalized material could also accelerate the electron-transfer rate, which resulted in a high ECL response signal amplification.

Liu and co-workers[75] fabricated a highly sensitive ECL immunosensing platform to monitor CEA expression by using ternary complexes of hemin-graphene-gold nanorods (H-rGO-AuNRs) as antibody carriers and QDs quenchers. Thanks to the high electrocatalytic activity of the ternary composite, H-rGO-AuNRs can not only reduce H_2O_2, which acts as the ECL coreactant, but also quench ECL intensity through the resonance energy transfer strategy between AuNRs and CdS:Eu QDs, which results in a double-quenching effect. The multiantibody amplification strategy that uses H-rGO-AuNRs as a nanocarrier possesses excellent performance for CEA detection with a detection limit of 0.01 pg mL^{-1}. Yuan's group synthesized a series of materials that included palladium nanowires,[76] manganese ion doped zinc oxide nanorods,[77] PdCu nanocubes that supported carbon nanohorns,[78] and core−shell Pd−Au hexoctahedrons,[79] which served as nanocarriers for loading antibodies.

DNA-Based Amplification. The electrochemical immune-DNA sensing platform consists of biorecognition events that capture targets and signal tags to amplify the detection. The DNA amplification approach, as a well-developed tool, provides good detection sensitivity and high specificity via competitive nucleotide hybridization for the development of ECL-based immunosensors. The RCA and self-synthesized nucleotide dendrimer were considered to be efficient strategies to improve analysis performance. Liang et al.[80] integrated RCA strategy and enzyme reaction to efficiently estimate the concentration ratio of two proteins (p-glycoprotein and glyceraldehyde 3-phosphate dehydrogenase). This sandwich-type ECL immunoassay was based on the conversion of proteins to nucleotide sequences and rolling circle amplification reactions to improve the detection limit and sensitivity. With the cascade amplification, the duplex-specific nuclease specifically cleaves sequences into coincident nucleotide sequences, which is followed by a reaction with the capture sequences on the surface of the electrode. Compared with conventional technologies, the competitive method-based ECL sensor exhibited an excellent performance in the identification of cancer cell drug resistance. In another work, a highly sensitive ECL immunosensor was generated by exponentially amplifying ECL signals with RCA and HCR for the simultaneous detection of the N-terminals of prohormone brain natriuretic peptide (BNPT) and cardiac troponin I.[81] The successful combination of an exponential amplification strategy, a $Ru(dcbpy)_3^{2+}$-modified complementary nucleotide sequence, and antibody-linked magnetic nanobeads leads to the efficient enhancement of the ECL response signal with high sensitivity. The simultaneous ECL platform showed a linear response range from 0.1 pg mL^{-1} to 8 ng mL^{-1} and from 0.2 pg mL^{-1} to 1 ng mL^{-1} for BNPT and troponin I, respectively.

To achieve good detection performance, DNA also can serve as an efficient linker for the amplification of the detection signal.[82] Huang et al.[83] synthesized silver-cysteine hybrid nanowires (SCNWs) to assemble DNA and fabricated a sandwich-type immunoreaction platform. This novel SCNW that had many functional groups was employed as a framework to assemble a large number of DNA-functionalized QDs, which led to the amplification of the ECL signal. On the basis of the specific sandwich ECL immunoassay, a good linear relationship was achieved from 1.0×10^{-12} to 5.0×10^{-10} g mL^{-1} for the sensitive detection of human immunoglobulin G (IgG).

DNA nanostructures provided many DNA duplexes via molecular self-assemble nanotechnology. DNA dendrimers contained highly branched structures that served as nanocarriers for the fabrication of the probe.[84] Wang et al.[85] adopted a biotin labeled DNA dendrimer as a carrier to load $[Ru(dcbpy)_2dppz]^{2+}$ and link *N*,*N*-diisopropylethylenediamine. The fabricated nanocomposite could bind with a streptavidin functionalized sandwich-type complex and induce a response signal from the ECL immunosensor. This proposed ECL immunosensor, with the signal amplification of a DNA dendrimer, exhibited a good sensitivity for *N*-acetyl-β-D-glucosaminidase detection.

Other Approaches. It is well-known that an antibody, as a core recognition molecule, plays a significant role in the fabrication of the high-performance ECL immunosensor. Conventional antibodies (polyclonal or monoclonal) possess lower binding activity with antigens after being labeled on the surface of nanomaterials.[86] Vast endeavors have been undertaken to screen new types of antibodies with more binding sites for the target. NBs, which derived from heavy-chain antibodies, are the smallest antigen-binding fragments and are obtained from the serum of camelids.[87] Due to their unique properties of high stability and good affinity, NBs are suitable for the development of various immunoassay systems. Li et al.[88] constructed a label-free ECL immunosensor for human procalcitonin determination based on affinity-matured NBs. The NBs were immobilized on a glassy carbon electrode as a procalcitonin capturing reagent and were attached onto silica-coated CdTe nanoparticles as a nanoimmunological label. The high affinity of NBs resulted in the establishment of a highly sensitive detection strategy with a wide linear range (0.01 to 20 ng mL^{-1}) for procalcitonin monitoring.

Mu et al.[89] combined protein functionalized gold-magnetic nanoparticles as a capture material and a $Ru(bpy)_3^{2+}$-modified phage displayed antibody as an ECL probe in the development of an ultrahighly sensitive ECL immunosensor. The authors claimed that the $Ru(bpy)_3^{2+}$-decorated phage displayed antibody produced a 20-fold amplification compared with a normal immunoassay. A wide linear detection range of 0.0001 to 200 μg L^{-1} was acquired for ricin detection.

DOI: 10.1021/acs.analchem.6b04281
Anal. Chem. 2017, 89, 138−156

IMMUNOSENSORS BASED ON PHOTOELECTROCHEMISTRY

On basis of two separate types of energies for excitation source and detection signal, photoelectrochemical (PEC) analysis, as a rapidly developed analytical technique, exhibits promising higher sensitivity due to the obviously reduced the background noise signal. Because it combines the merits of PEC analysis and immunoassay, the PEC immunoassay has aroused substantial interest in various fields. Recently, Xu and co-workers[90] provided a comprehensive review of recent advances in the cutting-edge research of PEC bioanalysis (183 references). Zhang's group[91] summarized the use of QD-based photoelectric conversion for biosensing applications (103 references). Herein, we focus on the recent progress of the PEC immunoassay with nanomaterial-enhanced, enzyme-based, and DNA-based signal amplification strategies as well as other interesting approaches.

Nanomaterial-Enhanced Amplification. Vibrantly photoactive nanomaterials have been demonstrated to be important elements in the analytical performance of PEC immunosensors.[92−94] A variety of semiconductor materials, including n-type[95,96] and p-type[97] semiconductors and their complexes,[98−100] has been utilized as photoactive species to design PEC immunosensors. Semiconductor nanocrystals, as near-infrared emitting materials, exhibit an intriguing potential for the construction of PEC immunoassay platforms due to their anti-interference capabilities. For instance, water-soluble near-infrared quaternary ZnCdHgSe QDs were utilized to fabricate a PEC interface by Li and co-workers.[101] The ZnCdHgSe QDs were integrated with a polymerized ionic liquid hybrid film modified indium tin oxide (ITO) electrode via layer-by-layer assembly for a highly sensitive PEC immunoassay of neuron specific enolase. Using a commercial white-light LED as an excitation source, the detection limit of this PEC immunosensor was able to reach 0.2 pg mL^{-1} by monitoring photocurrent variation.

Our group[102] proposed an ultrasensitive PEC immunosensing platform on the basis of a CdSeTe@CdS:Mn core−shell QDs-sensitized TiO_2 using CuS nanocrystals as signal amplifiers. As shown in Figure 4A, the TiO_2-modified ITO electrode was first assembled with CdSeTe alloyed QDs via polyelectrolyte-mediated electrostatic interaction and then deposited with CdS:Mn shells, forming the TiO_2/CdSeTe@CdS:Mn photoactive structure, which was used as a PEC matrix to immobilize the capture CEA antibody (Ab1). CuS nanocrystals were used to conjugate the signal CEA antibody (Ab2), which was employed as signal amplifier when the immunoreaction occurred. In this proposal, as illustrated in Figure 4B, the matrix structure of TiO_2/CdSeTe@CdS:Mn significantly increased the photocurrent response because of the presence of different semiconductors with different band gaps, which produced a mutual promotion effect to enhance the light absorption efficiency, prolong the lifetime of charge nanocarriers, and promote electron transfer. The signal amplifications of CuS nanocrystals were accomplished in two aspects. On the one hand, the photoactive property of CuS would competitively absorb the exciting light and expend the electron donor, resulting in an obviously weakened response of the photocurrent. On the other hand, CuS was employed as a nanocarrier to load numerous detection antibodies, which led to the depressed photocurrent intensity of the immunosensing platform. The proposed PEC immunosensor showed a very low

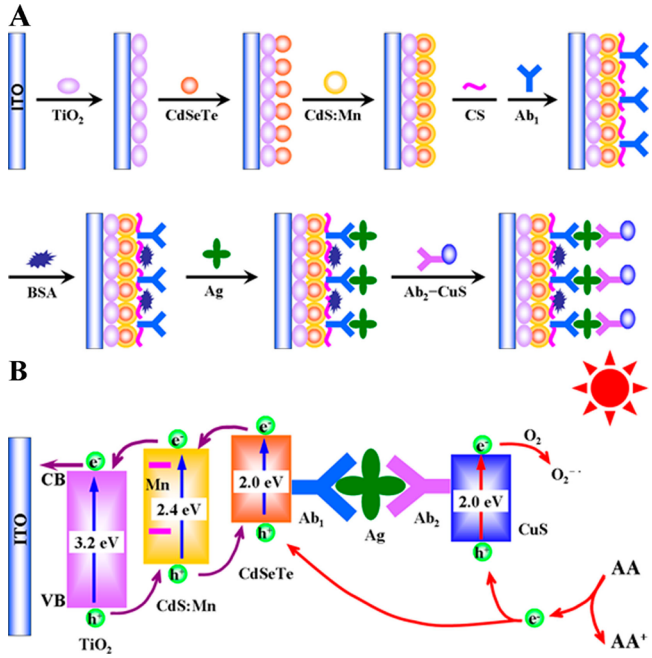

Figure 4. (A) Schematic diagram of the PEC immunosensing platform. (B) Photogenerated electron−hole transfer mechanism of the immunosensing system for the detection of a target antigen. Reproduced from Fan, G. C.; Zhu, H.; Du, D.; Zhang, J. R.; Zhu, J. J.; Lin, Y. *Anal. Chem.* **2016**, *88*, 3392−3399 (ref 102). Copyright 2016 American Chemical Society.

limit of 0.16 pg mL^{-1} and also exhibited good reproducibility and stability. Dai's group[103] described a silver iodide-chitosan (AgI-CS) nanotag-induced biocatalytic precipitation for a self-enhanced PEC immunoassay. In this work, AgI-CS nanoparticles acted not only as photoactive tags to improve the photocurrent intensity but also as peroxidase mimetics to catalyze the bioprecipitation reaction for signal amplification. Interestingly, the insoluble product in the bioprecipitation reaction skillfully served as an electron acceptor in this PEC system, which led to the great amplification of this PEC platform. The proposed PEC immunosensor showed an ultralow detection limit of 0.737 ag mL^{-1} for human interleukin-6. Very recently, the same group[104] reported on a fascinating potentiometric addressable PEC immunosensor for the sensitive detection of two biomarkers. In this work, two different photoactive materials, graphitic carbon nitride with an anodic photocurrent and AgI-CS with a cathodic photocurrent, were selected to label corresponding antibodies. Two different biomarkers (antigen) were immobilized onto the different disks of the modified electrode. The change in the photocurrent with the concentration of the target antigen at different critical voltages was utilized to selectively and simultaneously detect the target antigen. This proof of concept research demonstrated that this strategy could be used to detect multiple targets simultaneously.

Enzyme-Based Amplification. The application of an enzyme-based amplification to a PEC immunoassay has been demonstrated by the use of the in situ generation of an enzymatic hydrolysate as an electron acceptor or an electron donor, which may then trigger the PEC signal chain to assist in signal amplification.[105] Zhao and co-workers[106] recently exploited ALP tagged antibodies on AuNP/TiO_2 nanotube modified electrodes for an amplified PEC immunoassay of

DOI: 10.1021/acs.analchem.6b04281
Anal. Chem. 2017, 89, 138−156

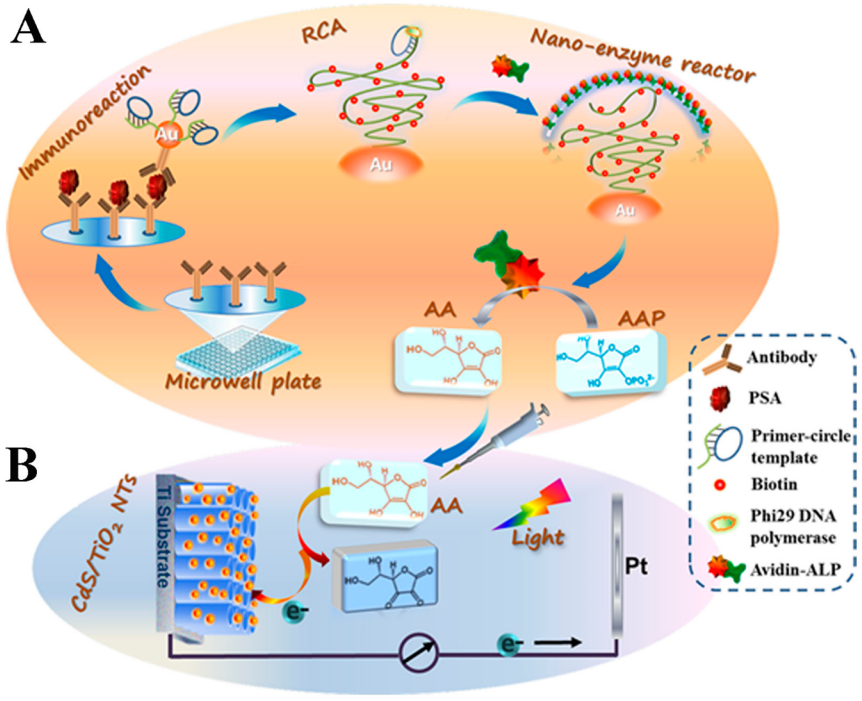

Figure 5. Schematic diagram of (A) an immunoreaction-induced ALP-based nanoenzyme reactor formation through RCA and (B) an enzymatic hydrolysate mediated hole-trapping in a CdS QD-sensitized nanotube array for the amplification of a photocurrent signal. Reproduced from Zhuang, J.; Tang, D.; Lai, W.; Xu, M.; Tang, D. *Anal. Chem.* **2015**, *87*, 9473−9480 (ref 110). Copyright 2015 American Chemical Society.

protein p53. In such a system, ALP possessed the enzyme activity to specifically catalyze ascorbic acid 2-phosphate to generate in situ ascorbic acid, which was employed as an efficient electron donor in the PEC platform. Using ALP and acetylcholine esterase (AChE) as tags, they also reported a general format for the simultaneous PEC immunoassay of dual cardiac biomarkers.[107] ALP and AChE were integrated into the PEC immunosensor through the sandwich immunoreaction and could catalyze ascorbic acid 2-phosphate or acetylthiocholine to ascorbic acid or thiocholine for sacrificial electron donation. Due to the proper PEC signal differentiation, this judicious approach achieved a dual assay of cardiac markers, which represents a potential application in clinical diagnostics and therapeutics. On the basis of the GOx catalytic generation of an electron donor coupled with the unique nanostructure of porphyrin-sensitized TiO_2, Tang's group[108] also designed a PEC immunoassay protocol for the sensitive detection of low-abundant proteins at a low potential.

DNA-Based Amplification. Although substantial progress in enzyme-based amplification strategies has been achieved in current PEC immunoassays, unfortunately, the enzyme-based labels suffer from inferior stabilities, and enzymatic activities are vulnerable to environmental impacts. More recently, DNA-based amplification strategies have been used for efficient signal amplification with stable and inexpensive tags for sensitive PEC immune analysis.[109] In these methods, various DNA amplification strategies, such as HCR, RCA, and nuclease-assisted target recycling, can be used to detect protein markers using DNA labeled antibodies. As an example, Tang's group[110] designed a new split-type PEC immunosensor for the detection of PSA based on RCA amplification (Figure 5). To achieve this design, thousands of repeated DNA sequences with many biotin moieties were synthesized on the nanogold tag through the RCA reaction. The formed DNA biotinylated concatamer acted as a powerful scaffold that reacted with avidin-labeled ALP. The enzymatic hydrolysate-enhanced PEC immune analysis was then completed using the CdS QD-modified TiO_2 nanotube array, which resulted in a high-throughput photocurrent signal. Furthermore, Wen and Ju[111] described an enhanced PEC proximity assay via DNA-labeled antibody. Upon the recognition of a labeled antibody-DNA (DNA-Ab1) to the target protein, the immune complex of the detection antibody-DNA (DNA-Ab2), the target, and the DNA-Ab1 was formed, which led to the proximity hybridization of the DNA-Ab2, the signal DNA-CdTe QDs, and the capture DNA, which produced a sensitized photocurrent. In addition, on the basis of electroactive purine nucleobases, a unique amplification probe that included DNA labeling for the sensitive PEC immune analysis of HIV-1 p24 antigen was reported by Xu's group.[112] In this work, following the sandwich immune reaction, the DNA labels can be released, and the dipurinization of DNA strands enables the oxidation of free nucleobases at the CdTe QD-modified ITO electrode. Such DNA tags induced PEC response amplification and displayed a general format for the PEC immune assay by means of DNA labeling.

Other Approaches. It is worth mentioning that a self-illuminated PEC system has also been explored.[113,114] As an example, Lu and co-workers[115] extended a split-type PEC immunosensor by coupling a peroxyoxalate self-illuminated platform for the detection of low abundance biomarkers with a digital multimeter readout. In addition, the oriented immobilization of an antibody is a promising method by which to increase the availability of immune elements by allowing an oriented binding with a minimal loss of affinity and specificity because an antibody's recognition sites are uniformly arranged and are exposed to the binding solution in an organized way. With the unique merits of NBs, such as their C-terminus ends being situated at the opposite site of the target (antigen) binding region, functional groups can be selectively conjugated at the C-terminus because this terminus is rarely involved in the

DOI: 10.1021/acs.analchem.6b04281
Anal. Chem. 2017, 89, 138−156

binding reaction. Inspired by this design, Liu et al.[116] described a label-free PEC immunosensor for the detection of neutrophil gelatinase-associated lipocalin (NGAL) through the use of a biotinylated anti-NGAL NB that was introduced to streptavidin-coated sensitized TiO_2 modified electrode. This PEC immunosensor exhibited a high binding capacity and a low detection limit of 0.6 pg mL^{-1}.

IMMUNOSENSORS BASED ON IMPEDANCE

Impedimetric and impedance derived immunoassays are inherently nondestructive and potentially sensitive indicators of interfacial change without labeling or amplification. Electrochemical impedance spectroscope (EIS) assays, including faradaic and nonfaradaic measurements, have been extensively utilized in immunoassays for the detection of low molecular weight targets,[117,118] biomarkers of protein,[119,120] cell,[121] and pathogens.[122,123] Similar to the vast majority of reported EIS assays, the faradaic EIS assay relies almost exclusively on measuring charge transfer resistance (R_{ct}) as a sensing parameter, which commonly results from a signal amplifying redox probe added in the electrolyte solution. Nonfaradaic EIS assays always utilize double layer capacitances (C_{dl}), phase (ϕ), and impedance ($|Z|$) as the sampling of functions in the absence of a redox probe in the electrolyte solution. During the past two years, both faradaic and nonfaradaic EIS assays were reported and some new methodologies, for example, impedance-derived electrochemical capacitance spectroscopy, based on frequency resolved immittance function electroanalysis,[124] were also investigated.

Taking advantages of label-free, simple, and fast analysis capabilities, EIS assays are widely utilized for the detection of small molecules, such as toxins,[125] hormones,[126] pesticides,[127] and feed additives.[128] For example, Shen and co-workers[129] established a simple immunosensor for testosterone detection based on an antitestosterone small single domain NB and EIS. Testosterone is a reproductive hormone that is produced by both men and women, plays a crucial role in normal cardiac function, and is a potential marker for numerous human diseases. As a result, this EIS immunosensor was successfully applied to detect testosterone with a detection limit of 0.045 ng mL^{-1}. Atrazine is a widely utilized pesticide in agriculture and exhibits adverse effects on human health. Through the use of an antibody-functionalized Cu-metal organic framework that conducts thin films, Kim and co-workers[130] described a conductometric immunosensor of atrazine with high sensitivity (detection limit of 0.01 nM) and specificity. Multiplex analyses with a single analyte based on polysilicon nanogap lab-on-chip[131] and a wearable biochemical sensor for monitoring alcohol consumption[132] were also reported by impedance measurement.

In addition to the focus of the above works on the detection of low molecular weight targets, various significant efforts have been devoted to the detection of protein biomarkers with an EIS immunoassay.[133] Human epidermal growth factor receptor 2 (ERBB2 or HER2), an important biomarker of breast cancer, was detected with EIS using a self-assembled monolayer of cysteamine.[134] Similarly, Siaj and co-workers[135] employed faradaic EIS as a sensitive technique to monitor the concentration of ovalbumin using chemical vapor deposited monolayer graphene film. Tissue polypeptide antigen,[136] lipoproteins,[137] and serum oncomarker CA125[138] in ovarian cancer patients were also sensitively detected by impedimetric and impedance derived immunoassays for early diagnostics. More significantly, Bueno and co-workers[124,139] investigated a frequency resolved immittance function analysis, which focuses on optimizing analytical potency and selecting and applying the most frequency-optimized reporter of interfacial change. From the same raw data sets, the new methodology, compared with traditional impedance analysis, requires no equivalent circuit analysis or prior assumption of response and obtains more important information, enabling an obvious reduction in assay acquisition and increased assay sensitivity. They successfully utilized this approach to effectively detect C-reactive protein, a clinical biomarker of protein.

To date, EIS immunoassays have also received more attention for the detection of cells[140] and pathogenic bacteria[141] or viruses.[142,143] Gao et al.[144] described a signal-off impedimetric immunosensor for the detection of *Escherichia coli* O157:H7. The immunosensor was fabricated by covalently immobilizing an anti-*Escherichia coli* O157:H7 antibody onto AuNPs and a self-assembled monolayer of a modified gold electrode. Marcali and Elbuken[145] exploited an impedimetric detection of agglutinated red blood cells in microdroplets with a droplet-based microfludic system. Yamamoto and co-workers[146] reported on a simple device for the detection of viruses between nanogap electrodes using nonlinear EIS. Depending on the differences in the impedance of virus types and virus concentration in the virus solution, the approach could distinguish and detect their approximate concentrations.

IMMUNOSENSORS BASED ON OTHER DETECTION TECHNIQUES

Recent achievements in electronic strategies have gained strong driving forces for the fabrication of EIs. By taking advantage of the electrochemical chips that combine advanced materials with signal transducing events to accurately transform biomolecular recognition elements to electronic signal outputs, field-effect transistors (FET) have aroused considerable interest in the field of EIs due to their convenient label-free strategy.[147] Tran and Mulchandani[148] reviewed recent progress in FET-based biosensors based on carbon nanotubes and graphene. From the authors' point of view, nanomaterial-based FET sensors provided good performance in ion, biomolecular, and small molecule detection. Aroonyadet et al.[149] synthesized an indium oxide nanoribbon (In_2O_3) on a Si substrate using two photolithographic masks for the fabrication of FET biosensors, which exhibited a high sensitivity to the pH change of the solution. As shown in Figure 6, the authors integrated sandwich-type immunosensing and enzyme-introduced pH reaction into the FET biosensors for model HIV-1 p24 protein detection. The fabricated biosensor possessed excellent sensitivity with a detection limit of 20 fg mL^{-1}, which is approximately 10^3-fold lower than the traditional immunoassay. In another study, Lee et al.[150] developed an ion-sensitive field-effect transistor (ISFET) immunosensor to detect the presence of proteins via the monitoring of pH changes. To enhance the sensitivity of ISFET, the thickness of the top gate oxide and the buried oxide in the transistor were precisely optimized. The dual gate ISFET platform showed good sensitivity to the hepatitis B surface antigen with a detection limit of 22.5 fg mL^{-1}.

In combination with the superior photocatalysis of TiO_2, Zhang et al.[151] prepared a renewable graphene-FET (G-FET) platform to monitor disease biomarkers. In this system, the G-FET chip was assembled by rGO and rGO/TiO_2 composites between the source and drain electrodes, followed by the

DOI: 10.1021/acs.analchem.6b04281
Anal. Chem. 2017, 89, 138−156

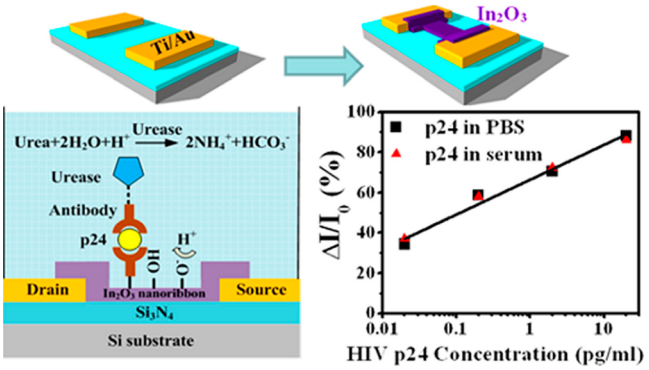

Figure 6. Fabrication processes of In_2O_3 nanoribbon biosensors and a schematic diagram of the streptavidin electronic ELISA. Reproduced from Aroonyadet, N.; Wang, X.; Song, Y.; Chen, H.; Cote, R. J.; Thompson, M. E.; Datar, R. H.; Zhou, C. *Nano Lett.* **2015**, *15*, 1943−1951 (ref 149). Copyright 2015 American Chemical Society.

immobilization of the capture antibody, the recognition of the antigen, and the recording of the electrical transfer curves. Notably, thanks to the photocatalytic activity of TiO_2, the chip surface could be cleaned via irradiation with a UV-light, which allowed the FET device to be reused multiple times.

Electrically driven systems effectively generate microflows to modulate fluid transport across the detection device.[152] Alternating current electrohydrodynamic (ac-EHD) as a fascinating driven fluid system can enhance analyte transport, remove nonspecific substances, and minimize background noise, as well as reduce total assay time.[153] Vaidyanathan et al.[154] demonstrated a sensitive protein sensor that was based on ac-EHD and was coupled to a recombinant nanoyeast-scFv as a capture antibody. In detail, the nanoyeast-scFv, the antigen, and the QD functionalized antibody formed a sandwich-type complex at the surface of the device. Then, the fluorescence intensity was recorded with a confocal microscope to quantitatively detect *Entamoeba histolytica* antigens. This work used ac-EHD to enhance the probe−target interaction and to control the reaction time of the capture and detection steps within 5 min. Han and Park[155] designed an immunoreaction sensing platform by employing optically induced EHD flows to improve antibody−antigen recognition efficiency and optoelectrofluidity to enhance the performance. Thus, the electrokinetic approaches are potentially promising for the rapid analysis in biological fields.

The potentiometric assay is an important electrochemical sensor and has been widely used for ion detection.[156] The introduction of the immunoassay into potentiometric sensors has extended the application of the monitoring of biomolecules. Zhang et al.[157] described an ultrasensitive potentiometric immunosensor for troponin complex detection that used open circuit potentiometry (OCP). The charge of the working electrodes, which included emulsion-polymerized polyaniline/dinonylnaphthalenesulfonic acid (PANI/DNNSA), was mediated through electron and charge transfers that were generated by enzymatic reactions, leading to potential variations. The potentiometric sensors exhibited good sensitivity with a detection time that was less than 10 min. Figueiredo et al.[158] measured the variations in OCP to direct the electrical detection of nonstructural protein 1 (NS1) by using egg yolk immunoglobulin (IgY) as recognition reagent. The potentiometric sensor consisted of an anti-NS1 IgY antibody modified working electrode, a platinum wire counter electrode, and an Ag/AgCl reference electrode, which could analyze NS1 via the monitoring of the negative charge of the gold electrode. The proposed biosensor showed a fast response and good sensitivity in the range of 0.1 to 10 mg mL^{-1} for NS1 detection. The direct and rapid strategy can be generalized to the detection of many biomolecules.

In the development of a noninvasive and label-free tool for biomarker detection, piezoelectric transducers, consisting of a quartz crystal microbalance (QCM) as a fascinating device, play a critical role in the fabrication of immunosensors.[159] Luo et al.[160] modified the antibody on the QCM surface to construct a piezoelectric immunosensor for the quantitative detection of thrombomodulin. An anti-antibody functionalized AuNP can bind to the QCM surface through an antigen−antibody reaction, and the binding was noticeably blocked by the immobilized thrombomodulin because of a strong steric hindrance effect, which caused a change in the resonant frequency. The relative frequency shift showed a good linear relationship with thrombomodulin concentration in the range from 10 to 5000 ng mL^{-1}. Deng et al.[161] described a high-sensitivity piezoelectric immunosensor that was based on a biotinylated graphene oxide−avidin complex functionalized QCM. The integration of flow-based strategies with a QCM chip exhibited good performance and less analysis time without prefunctionalization steps. In another work, March et al.[162] developed a high fundamental frequency (HFF) QCM chip to monitor carbaryl and thiabendazole. The novel HFF sensor utilized the phase/mass relationship to increase the frequency, which enabled sensitive mass sensing. The assay achieved a detection limit of 0.14 and 0.06 $\mu g\ L^{-1}$ for carbaryl and thiabendazole, respectively. Future efforts will focus on the integration of new nanomaterials with the surface of electrode and the miniaturization of the detection device to provide a more suitable real-time detection.

■ NOVEL DEVICES AND PLATFORMS

With the achievements of functional nanomaterials and nanotechnology, EIs have shown excellent performance for target detection.[163] Although enormous improvements in detection sensitivity and accuracy have been achieved, the new functional nanomaterial-based EIs require cumbersome instruments or devices to operate, analyze, and display response signals.[164] The pursuit of real-time, economical, portable, and easy-to-construct devices has focused on the miniaturization of EIs, such as portable readout instruments[165] and paper-based fluidics.[166] The integration of an emerging sensing platform into an immunoassay strategy shows great potential application in numerous fields, such as food quality control, drug screening, and clinical diagnostics. The following are some examples of novel sensing platforms and devices for the construction of EIs.

Microfluidic and Paper-Based Platforms. The miniaturization of EIs on microfluidic platforms can not only overcome the limitations of conventional approaches, including the consumption of large volumes of reagents and the requirement for long detection times, but also extend the application of immunosensors as POC tools.[167−169] Coupled with different fabrication strategies, various microfluidic-based devices were constructed for virus and protein detection.[6] Li and Liu[170] reported a microfluidic paper-based origami biosensor for HIV p24 antigen and rabbit IgG detection. The researchers fabricated the microfluidic paper-based devices by using cellulose paper via taping and origami. The paper piece with a carbon working electrode was directly decorated with zinc

DOI: 10.1021/acs.analchem.6b04281
Anal. Chem. 2017, 89, 138−156

oxide nanowires (ZnO NWs), which could enhance the electrode surface area and immobilize the probe proteins, boosting the detection performance of the device. The microfluidic paper-based origami biosensor had fewer operation steps and a shorter assay time and exhibited an ultralow detection limit of 60 and 300 fg mL^{-1} for rabbit IgG and the HIV p24 antigen, respectively.

Sun et al.[171] presented a multiplexed enzyme-free immunodevice that combined ZnO nanorods (ZNRs) with an rGO decorated paper electrode. In this work, ZNRs/rGO could not only increase the number of binding sites for the conjugation of capture antibodies but also improve the electronic transmission rate. Furthermore, bovine serum protein-stabilized silver nanoparticles served as excellent signal labels and could catalyze the reduction of H_2O_2, which amplified the strategy signal. The microfluidic-based strategy possessed good performance for the detection of human chorionic gonadotropin, PSA, and CEA with high sensitivity.

The combination of biofuel cells (BFCs) and microfluidic-based devices with good performance has drawn increased attention owing to its self-power without external sources and its simple fabrication process.[172] Li et al.[173] developed a BFC-based immunoassay that was constructed with microfluidic devices for CEA detection. The sensor was constructed with silver nanoparticles and a functionalized graphene modified paper electrode as the substrate for the anti-CEA antibody, CEA-AuNP-glucose dehydrogenase (CEA-Au-GDH), and PtNi alloy−bilirubin oxidase (PtNi−BOD). In the presence of glucose and O_2, CEA-Au-GDH and PtNi−BOD acted as biocatalysts to enhance glucose oxidation and O_2 reduction, which induced a self-powered signal response. This proposed BFC-based microfluidic device possessed a low detection limit of 0.7 pg mL^{-1} for CEA. In another work, Wu et al.[174] proposed the use of a paper-based EI for the sensitive detection of the carbohydrate antigen 15-3 (CA15-3) by employing a visible-light-enhanced BFC. The paper-based immunoassay was powered by BFC that consisted of a gold nanocomposite modified paper electrode and GDH functionalized gold−silver bimetallic nanoparticles. The electron amount was determined by the GDH concentration, which finally related to the concentration of CA15-3. According to the amperometric signal, a highly sensitive detection can be achieved in the range of 0.01 to 50 U mL^{-1} for CA15-3.

Thanks to the inclusion of a hybridization chain reaction, the RCA strategy can repeat a nucleotide sequence within a short time period, which remarkably enhanced the detection signal.[175−177] Wu et al.[178] fabricated a paper-based cascade signal amplification device for the sensitive detection of IgG antigen via the RCA technique. The gold-paper electrode served as a working electrode to load the capture antibodies, followed by an RCA procedure that contained tandem-repeat sequences. In addition, the oligonucleotide-functionalized carbon dots served as a signal recognition material and could successfully assemble on an RCA product, which dramatically improves the sensitivity. A wide linear range from 1.0 fM to 25 pM was obtained for human IgG detection.

Microfluidic bioreactors as an emerging device can produce biomimetic units and can respond to changes in microenvironment; these devices have received increasing attention.[179] Thus, the construction of microfluidic bioreactors with integrated EIs can assist in the study of biomarker changes at the cellular level. Riahi et al.[180] introduced a microfluidic-based electrochemical immunoassay for the sensitive detection of cell-secreted biomarkers (transferrin). The microfluidic chip coupled with an immunoassay was carried out by an automated valve controller system. The microfluidic platform could control the magnetic microbead loading and binding steps, as well as the subsequent antibody−antigen interactions. The automated on-chip immunoassay showed a low detection limit of 0.03 ng mL^{-1} for transferrin. More importantly, magnetic microbeads could immobilize with different antigens, which resulted in the application of multiple biomarkers that employed the automated sensor.

A sequential injection analysis combined with a microfluidic-based bead-trapping device has been established as a powerful analytical tool based on the bidirectional movements of carrier microbeads.[181] Our group[182] described a novel microfluidic beads-trapping device that was generated with polydimethylsiloxane soft lithography technology. In this design, the pillar array and the pneumatically driven flexible membrane were employed for bead-trapping and bead-releasing, respectively. This device has been successfully demonstrated for detecting mouse IgG with a low detection limit of 0.1 ppb.

Electrode Arrays and Chips. To pursue a high throughput analysis and an ultrasensitive multiplexed electrochemical measurement, many endeavors have been performed to fabricate array architectures for the realization of detection goals in a POC and a real time manner.[183,184] An EI array that is integrated with nanomaterials is a promising platform for a fast, accurate, and multiplexed analysis in many research fields.[185,186] Chiriacò et al.[187] produced a lab-on-chip platform for multianalysis based on EIs. The immunochip contained four separate microfluidic sensing areas that were decorated with gold interdigitated microelectrodes. This biochip allowed for multiplexed detection without any pretreatment, which enabled a quick screening in gynecological outpatient clinics. Otieno et al.[188] described a multiplex immunoarray that featured a semiautomated microfluidic device to measure isoforms of parathyroid hormone-related peptide. An antibody-modified 8-electrode array was used as a capture element to recognize peptide analytes, which then formed a sandwich-type structure with an enzyme/antibody conjugated magnetic bead. The assay provides good sensitivity for the simultaneous monitoring parathyroid hormone-related peptide isoforms within 30 min.

A bipolar electrode (BPE) does not need to directly connect with external power to facilitate the construction of a chip platform.[189] Particularly, the integration of BPE with an ECL approach, which does not require a light source, is ideally suitable for the miniaturization of the detection device and the achievement of multiplexed detection. Wu et al.[190] demonstrated a visual electrochemical platform for the sensitive detection of cancer biomarkers via the integration of driving electrodes and a closed BPE array into a multichannel chip. In this glass substrate-based chip, the detection channel and sensing channel were linked by parallel BPEs that loaded gold film on the cathodes and $Ru(bpy)_3^{2+}$/tripropylamine on the anodes. Antibody-functionalized thionine/silica nanoparticles were used as both recognition probes and electrochemical tags for the visual detection of PSA and AFP. Furthermore, the proposed device could simultaneously detect eight samples, which is suitable for the construction of a multiplex analysis in one chip. Zhai et al.[191] also fabricated a nanoscale multichannel BPE array for AFP and CEA detection. The author successfully embedded a nanochannel into the inner channel of a poly(ethylene terephthalate) membrane that was decorated with gold nanofibers. This BPE-based device showed a great

DOI: 10.1021/acs.analchem.6b04281
Anal. Chem. 2017, 89, 138−156

potential for multianalysis. In another study, Shi et al.[192] designed a BPE sensing platform that coupled anodic dissolution with an ECL sensor for the detection of cancer cells. AuNPs were assembled at the anode working pole, which worked as a catalyst for the luminol/H_2O_2 reaction and as a seed for Ag nanoparticles deposition. Then, the ECL signal was quenched due to resonance energy transfer and a decrease in the electrode conductivity. After the application of sufficient potential on BPE, the Ag started to dissolve, and the ECL signal began to recover. Cells incubated on BPE were related to the ECL anodic dissolution time.

Kadimisetty et al.[193] developed a microprocessor-controlled microfluidic immunoarray for a multiplexed application. The programmable microprocessor controlled six separate micropumps that operated the microfluidic channels. The pyrolytic graphite detection chip was embedded in a microfluidic chamber and was decorated with an antibody functionalized carbon nanotube that could specifically recognize the detection proteins. The proposed microfluidic immunoarray showed excellent performance in the simultaneous detection of the four prostate cancer protein biomarkers within 36 min. The combination of the automated microprocessor with a microfluidic immunoarray provided a promising idea for POC devices.

Due to its capacity for simultaneous measurements of multiple cells, vertical nanowire electrode arrays (VNEAs) are considered to be powerful techniques for intracellular recordings.[194,195] Nasr et al.[196] prepared an EI that was based on VNEA for the detection of glial fibrillary acidic protein (GFAP), which is a major astrocytic structural component. The VNEA chip was modified with 3-aminopropyl-triethoxysilane, which allowed the use of immobilized GFAP. The response of VNEA to the concentration of the capture antibody was evaluated with the fabrication of an electrochemical cell. This proposed intracellular detection approach exhibited good detection sensitivity for GFAP in the range of 2.9 ng mL^{-1} to 290 μg mL^{-1} in a living cell.

The emergence of 3D printing technologies provides new ideas and opportunities for the design of biosensor systems.[197−199] Rusling's group[200] printed a sample/reagent delivery system for the construction of a supercapacitor-powered ECL immunoarray. The printed device, which consisted of reservoirs, was used to deliver the sample/reagent to a screen-printed electrode array for incubation, followed by the removal of the reagents with gravity flow. The microfluidic immunoarray was powered by a supercapacitor to supply voltage for the ECL process that could simultaneously measure three prostate cancer biomarkers with a detection limit of 300−500 fg mL^{-1}. Furthermore, the ECL-based assay was low-cost (~€0.50 each sample) and easy to operate, with an analysis time within 35 min.

Hand-Held Devices. The fabrication of portable sensors has attracted scientists' and engineers' interests because it provides a real-time readout and uses a device to achieve multiplexed measurements, especially in low-resource settings. Hand-held instruments are miniaturized electrochemical devices that can produce a real-time signal and have shown promising applications in POC testing.[201] Thus, the inexpensive diagnostic platforms that have employed portable devices as readers for reliable measurements include glucose meters,[202,203] pH meters,[204] and smartphones.[205,206] The major challenge is the conversion of a biomolecular recognition event into a measurable numeric signal by a hand-held device. To address this issue, many attempts have been made to use enzyme and catalytic nanoparticles, which can transfer the substrate into glucose, a gas, or an acidic substance. Here, we focus on the recent research on hand-held instrument platforms.

pH Meter. In a pH meter-based electrochemical sensor, the key concept of sensor design was the conversion of the analyte concentration into a hydrogen ion concentration response signal, followed by the utilization of a pH meter to provide a reliable numeric readout. The enzymes, including acetylcholinesterase and GOx, served as powerful tags since they could efficiently catalyze the substrate into an acidic substance that could elicit the response of a pH meter in the fabrication of an electrochemical sensor. Thus, the analytical performance of the electrochemical sensor was related to the activity of the enzyme and the sensitivity of the pH meter. To provide evidence of the sensor effectiveness, Kwon et al.[207] designed a sensitive and facile method for cardiac marker troponin I determination via pH meters. Antibody modified magnetic nanoparticle clusters were prepared to capture the target protein, and sandwich-type immunocomplexes were then formed from antibody-functionalized acetylcholinesterase. In the presence of acetylcholine, the enzymatic hydrolysis (acetic acid) could induce a decrease in the pH, which was measured by a pH meter. The proposed sensor achieved a detection limit of 10 pg mL^{-1} for troponin I.

Inspired by the hand-held platform, our group[208a] combined organic−inorganic hybrid nanoflowers with a pen-size pH meter for the sensitive analysis of food pathogens (Figure 7).

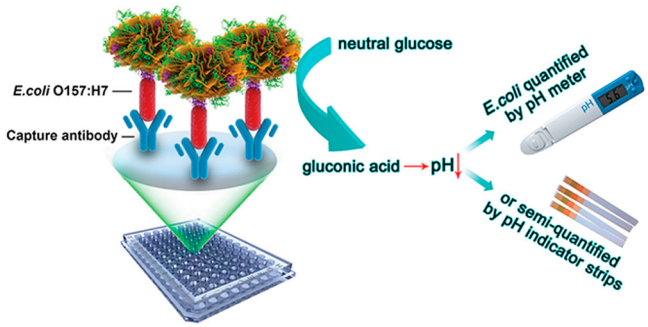

Figure 7. Illustration of the organic−inorganic hybrid nanoflowers-based immunoassay for the detection of *Escherichia coli* O157:H7 with a hand-held pH meter. Reproduced from Bioinspired Synthesis of All-in-One Organic−Inorganic Hybrid Nanoflowers Combined with a Hand-held pH Meter for On-Site Detection of Food Pathogen, Ye, R.; Zhu, C.; Song, Y.; Lu, Q.; Ge, X.; Yang, X.; Zhu, M.; Du, D.; Li, H.; Lin, Y. *Small* Vol. *12*, Issue 23 (ref 208a). Copyright 2016 from Wiley-VCH with permission.

The hybrid nanoflowers were synthesized via a mimetic biomineralization process by gently mixing concanavalin A, GOx, and $CaHPO_4$ solutions. The hybrid nanoflowers possess dual functions as both recognition units for *Escherichia coli* O157:H7 and signal tags for enzymatic amplification. After an immunoreaction procedure for *E. coli*, GOx in nanoflowers can catalytically oxidize the glucose to gluconic acid, which is easily measured with a pH meter. Under the optimal conditions, the established platform possessed good performance for *E. coli* detection in the range of $10-10^6$ CFU mL^{-1}. In another design,[208b] invertase was used to replace the GOx in the hybrid nanoflower and a personal glucose meter was used for the quantification of *E. coli*. Li's group[209] also developed a general enzyme-linked immunosorbent assay by employing a hand-held

DOI: 10.1021/acs.analchem.6b04281
Anal. Chem. 2017, 89, 138−156

pH meter as signal readout for the quantification of human oncogenic protein. Interestingly, the pH measurement-based sensor showed a 14-fold enhancement of the sensitivity of a traditional assay. Thus, the pH meter-based immunosensor offers new opportunities for the application of the existing commercially available enzyme-linked immunosorbent assay for routine analysis.

Glucose Meter. The personal glucose meter (PGM) is a common device for POC testing in household scenarios because of its reliable quantitative results and ease of use. Recently, functional DNA sensors that were coupled with a general PGM readout were designed for the sensitive detection of many targets, such as recreational drugs[210,211] and protein biomarkers.[212,213] Thus, the remarkable achievements in PGM-based immunosensors have been addressed below.

Tang's group[214] adopted a competitive-type immunosensing platform for mycotoxin detection that was based on polyethylenimine-coated mesoporous silica nanoparticles (PEI-MSN). To construct this immunosensor, PEI-MSN worked as a container that carried numerous glucose molecules, and an antibody-labeled AuNP (mAb-AuNP) served as a gatekeeper to modulate the on−off functions of pores. The mAb-AuNP would be replaced by aflatoxin B1 through an antigen−antibody reaction, causing the release of glucose, which could be quantitatively detected via a commercial PGM. Under this circumstance, the competitive-type displacement immunosensing platform showed good sensitivity for aflatoxin B1 detection in the range of 0.01 to 15 μg kg^{-1}. In another study, the authors[215] demonstrated a homogeneous immunoassay strategy for the sensitive monitoring of biotoxin by employing a magnetic mesoporous $NiCo_2O_4$ nanostructure (MMB) as the support, a poly(ethylenimine)-coated polystyrene microsphere (PEI−PSMS) as molecular gate, and glucose as the detection signal of PGM.

Liposomes, as functional vesicles, can easily encapsulate biomolecules for signal amplification in biosensors.[216,217] Our group[218] developed a low-cost immunosensor to quantitatively detect disease biomarkers on the basis of glucose encapsulating liposomes (GEL) and antibody functionalized magnetic Fe_3O_4 nanoparticles (Ab-Fe_3O_4). The model analyte was captured by Ab-Fe_3O_4 and antibody-conjugated GEL to form a sandwich structure that was separated with a magnet. After lysing the bound liposomes, glucose was released and monitored with a portable PGM. The PGM response increased with the addition of biomarker concentration (phospho-p53[15]) in the linear range of 0.3−20 ng mL^{-1}. Yang's group[212] designed a general liposome-linked immunosorbent sensor that used a PGM for a sensitive readout, coupled with antibody-functionalized capture magnetic beads and enzyme-encapsulated liposomes. A liposome can quickly be broken with surfactant Triton X-100 and can release invertase, which converts the substrate to glucose and causes a signal change in the sensor. It was demonstrated that C-reactive protein could be analyzed by PGM with a detection limit of 0.30 nM.

Wang et al.[219] proposed a novel strategy for myoglobin detection via the utilization of an invertase−aptamer conjugate as signal amplification element. The introduction of myoglobin will boost the formation of an "antibody−myoglobin−aptamer−invertase sandwich" complex to catalytically hydrolyze sucrose to glucose, leading to a tremendous detection signal that is recorded by a PGM. By employing a different aptamer and antibody, the PGM-based strategy could be easily extended to the portable detection of a nonglucose target.

Pressure Meter. A physical parameter (gas pressure) signal can be converted into a reliable numeric readout with a pressure meter; thus, the integration of a gas-generation reaction and a biomolecular recognition component can be considered a promising strategy for POC testing that satisfies the requirement of simplification and miniaturization. Yang's group[220] successfully transferred an antigen−antibody specific reaction into a pressure signal for protein biomarker analysis. This sensing platform was combined with a sandwich immunosorbent assay that had pressure-based biosensors (termed PLISA). The sandwich complex was formed between immobilized capture antibodies, biomolecular analytes, and catalase or Pt nanoparticles for the functional detection of an antibody. The introduction of H_2O_2 can initiate an enzyme-catalyzed reaction to generate gas, which results in an obvious pressure change that can be recorded with a portable pressure meter. Using the PLISA technology, a gas concentration-dependent pressure platform contains two important signal amplification factors and can achieve an excellent performance for the detection of protein biomarkers without optical or magnetic field noise. In their other work, the authors[221] reported a POC testing strategy for C-reactive protein detection by translating the biomolecular recognition event into a pressure response, coupled with the excellent catalytic ability of Pt nanoparticles.

Digital Multimeter. As an alternative to an expensive electrochemical workstation, a digital multimeter (DMM) provides reliable quantitative readings of amps, volts, and ohms, which opens a new horizon for the construction of EIs. Tang's group[222] described a DMM-based immunosensing system for the sensitive determination of a biomarker by using a capacitor/DMM electronic circuit and an enzymatic catalytic reaction. The sandwich-type structure was fabricated with a capture antibody, protein biomarker, and GOx-conjugated detection antibody. Due to the enzymatic reactions, two half-cells that were linked by a salt bridge had different ratios of $[Fe(CN)_6]^{3-}/[Fe(CN)_6]^{4-}$ and thus produced a voltage that charged a capacitor. Finally, DMM was utilized as an electrochemical detector to measure instantaneous current when the capacitor discharged. The DMM-based platform showed a dynamic detection range from 0.05 to 7 ng mL^{-1} for PSA. Shu et al.[223] integrated the sandwich-type immunoreaction, chemiluminescence self-illuminated system, and DMM-based current detection assay for the fabrication of a split-type photoelectrochemical sensing platform. In this detection platform, H_2O_2 was generated by the oxidation of glucose and then H_2O_2 triggered the chemiluminescence, which could induce rGO-doped $BiVO_4$ to produce a voltage. Several advantages of the DMM-based immunosensing platform are shown below. First, the proposed immunoassay affords a high sensitivity that results from an antibody−antigen reaction and enzymatic amplification. Second, DMM is simpler and cheaper compared to a conventional electrochemical workstation. More importantly, this platform can be extended to detect other biomolecules by changing the biorecognition elements.

Smartphone. The pervasive usage of the smartphone makes it integral in many fields of our modern life. By taking advantage of the smartphone, researchers have attempted to develop biosensors to minimize the device size, reduce the cost of the system, and simplify the electronic design.[224−226] Owing to its advanced computing capability and the inclusion of a high-resolution camera, a smartphone can be employed as a screen display,[227] data analyzer,[228] and signal detector.[229,230]

DOI: 10.1021/acs.analchem.6b04281
Anal. Chem. 2017, 89, 138−156

Smartphone-based biosensors will also enable the real-time monitoring and transfer of information to a digital network. Some examples of smartphone-based EIs for portable healthcare diagnostics are introduced below.

Nemiroski et al.[231] designed a universal mobile electrochemical detector (uMED) for glucose, heavy metals, sodium, and malarial antigen and employed a mobile phone as an input button and a screen display. This low-cost device contains three parts: an external electrode (screen-printed electrode, ion-selective electrode, or test strips) as the reaction medium, an uMED as a data analyzer, and a mobile phone as an input button and a modem. The fabricated uMED device can process and transmit data automatically, requires few resources, and accurately performs analyses. The proposed device performed an enzyme-linked immunosorbent assay for malarial antigen detection. Furthermore, some sophisticated diagnostic testing techniques could be simplified in this uMED platform. Aronoff-Spencer et al.[232] presented a smartphone-based platform to detect the antihepatitis C virus antibody by coupling dual-affinity yeast biobricks. On the basis of an antigen-based antibody capture strategy and enzymatic reactions, the streamlined detection platform showed excellent sensitivity for antihepatitis C virus antibody with a detection limit of 2 nM.

To miniaturize the sensing device, an electrochemical detector was attempted to be embedded into a smartphone for signal processing and data analysis. Fan's group[233] constructed a low-cost sensing strategy for clenbuterol monitoring by combining a homemade mobile electrochemical chip. This electric field-driven acceleration approach could not only lower the immune competition time but also enhance the detection sensitivity. MWCNTs were used to decorate screen-printed electrodes and to immobilize the capture antibody. Then, a competitive immunoassay was performed by adding clenbuterol and HRP-coupled clenbuterol. The current signal was significantly amplified via enzymatic reactions. The competitive immunoassay exhibited an electric field-driven acceleration, was finished within 6 min, and showed a wide linear range from 0.3 to 100 ng mL^{-1} for clenbuterol detection.

CONCLUSIONS AND PERSPECTIVES

In the past two years, thousands of research papers were published regarding the development of EIs. We have summarized recent remarkable progress in the design and construction of novel EIs, with a specific focus on emerging signal amplification strategies and new devices. By using functional nanomaterials, a DNA/enzyme amplification approach, and new electroanalytical techniques, EIs are both sensitive and selective, especially in the simplification and miniaturization of devices, making them ideally suitable for POC diagnosis.

On the basis of the literature discussed in this Review, the sensitivity and selectivity of EIs can be improved as follows: (1) the development of proper electrode-modified materials with novel properties to improve the electrical conductivity and increase the specific surface area, (2) the use of novel functional nanomaterials that serve as antibody carriers, catalysts, and signal tags, (3) the use of a DNA or enzyme-based amplification approach, and (4) the development of a new immune recognition element that requires a high binding affinity for the binding target. On the other hand, the integration of EIs into microfluidic and paper-based platforms, hand-held devices, arrays, and chips can be achieved via high automation, simplicity, and miniaturization and promotes the commercialization of devices in the near future.

Although the desirable advantages in current electrochemical immunoassays are obvious, there are still some significant challenges and obstacles in this field. For instance, the stable and effective integration of the recognition event (antibody) into the electrochemical analytical system is the key factor for the establishment of a successful EI. Because of the macromolecular structure and the nonconductive properties of the antibody, it is often necessary to conjugate the antibody to functionalized nanomaterials, which will inevitably increase the complexity, cost, and time of immunosensor construction. Furthermore, due to the complicated preparation process of EIs and the complexity of the immunoassay, the reproducibility and stability of EI are susceptible. Particularly, environmental conditions can influence the performance of EIs with antibodies or enzymes. Most importantly, the practical sample analysis in complex matrices or in an online analysis of implanted organisms is also a challenging task in the development of electrochemical immunoassays. Thus, future endeavors should directly focus on solving these problems.

With the further development of science and technology, tremendous opportunities and broad prospects for the development of EIs have emerged. Coupling newly developed nanomaterials with other recognition elements such as nanobodies, peptide aptamers, and protein receptors would open up new avenues for electrochemical immunoassays and further extend their applications. Especially, the use of multifunctional nanomaterials with rich nanostructures could improve the performance of a sensor and increase the sensitivity and the accuracy of the sensor. Furthermore, the integration of an emerging sensing platform into EIs shows promising applications in personalized POC measurements. 3D printing technologies are capable of improving the reproducibility and stability of EI by precise device production processes with fast design-to-object multiplex capabilities and different analytical formats. In combination with 3D printing technologies, the immune recognition event can be converted into a measurable digital signal by hand-held, wearable, and implantable devices, for example, smartphones and wrist watches. With the advantages of real-time monitoring and the transfer of information to a big data network, these EI devices will pave the way for a new generation of analytical devices in the POC field, which is critical for homeland security, food safety, infectious disease control, and personal health applications. We, therefore, envision that EIs will certainly play important roles in future biosensing.

AUTHOR INFORMATION

Corresponding Authors

*E-mail: Annie.du@wsu.edu.

*E-mail: Yuehe.lin@wsu.edu.

ORCID

Yuehe Lin: 0000-0003-3791-7587

Author Contributions

§W.W. and X.Y. contributed equally.

Notes

The authors declare no competing financial interest.

Biographies

Wei Wen is an associate professor at College of Chemistry and Chemical Engineering in Hubei University. He received his Ph.D. degree in biomedical photonics from Huazhong University of Science

DOI: 10.1021/acs.analchem.6b04281
Anal. Chem. 2017, 89, 138−156

and Technology in March 2014. Currently, he is a visiting scholar in the School of Mechanical and Materials Engineering at Washington State University under the supervision of Prof. Yuehe Lin. He has coauthored over 40 peer-reviewed publications. His scientific interests focus on development of functional nanomaterials for electrochemical sensors and biosensors.

Xu Yan received his master's degree from Nanjing Agricultural University, China, in 2013, and then entered the Ph.D. program in Prof. Xingguang Su's group at Jilin University (P. R. China). Currently, he is working as a joint Ph.D. student in Prof. Yuehe Lin's group at Washington State University. He has coauthored over 20 peer-reviewed publications. His research interests mainly focus on the development of functional nanomaterials for fluorescent and electrochemical biosensors.

Chengzhou Zhu graduated with a BS degree in chemistry from Shandong Normal University (P. R. China) in 2007. He joined the group of Prof. Shaojun Dong at the Changchun Institute of Applied Chemistry and received his Ph.D. degree in January 2013. Since then, he did postdoctoral work with Prof. Alexander Eychmüller supported by the Alexander von Humboldt Foundation in Dresden University of Technology. Currently, he is an Assistant Research Professor in Prof. Yuehe Lin's group at Washington State University. He has coauthored over 90 peer-reviewed publications, with citations of ~4400, and an h-index of 31. His scientific interests focus on nanomaterial-based electrochemical energy and analytical applications.

Dan Du received her Ph.D. in Analytical Chemistry from Nanjing University in 2005. She joined Central China Normal University in 2005 and was promoted to Full Professor in 2011. Currently, she is a Research Professor in Washington State University. Her research interests include functional nanomaterials for biosensing and drug delivery. Dr. Du has published over 150 papers, with citations of ~6100, and an h-index of 50.

Yuehe Lin is a professor at Washington State University and a Laboratory Fellow at Pacific Northwest National Laboratory. He has been actively working in the nanotechnology area, particularly in the development of new biosensors and bioelectronic devices and nanomaterials for biomedical diagnosis and drug delivery. His other research activities include synthesizing functional nanomaterials for energy and environmental applications. Dr. Lin has published ~400 papers, with 33 000 total citations and an h-index of 96, according to Google Scholar. He was listed as a highly cited researcher in chemistry on Thompson Reuters's lists in 2014, 2015, and 2016.

■ ACKNOWLEDGMENTS

This work was supported partially by Grant U01 NS058161 from the National Institute of Health Office of the Director (NIH OD) and the National Institute of Neurological Disorders and Stroke (NINDS) and Grant R21 OH010768 from the CDC/NIOSH. Its contents are solely the responsibility of the authors and do not necessarily represent the official views of the federal government. We would like to acknowledge Drs. Chenzhong Li and Jianping Lei for reading the manuscript and helpful comments.

■ REFERENCES

(1) Rezaei, B.; Ghani, M.; Shoushtari, A. M.; Rabiee, M. *Biosens. Bioelectron.* **2016**, *78*, 513−523.
(2) Rackus, D. G.; Shamsi, M. H.; Wheeler, A. R. *Chem. Soc. Rev.* **2015**, *44*, 5320−5340.
(3) Kokkinos, C.; Economou, A.; Prodromidis, M. I. *TrAC, Trends Anal. Chem.* **2016**, *79*, 88−105.
(4) Wan, Y.; Su, Y.; Zhu, X.; Liu, G.; Fan, C. *Biosens. Bioelectron.* **2013**, *47*, 1−11.
(5) Lim, S. A.; Ahmed, M. U. *RSC Adv.* **2016**, *6*, 24995−25014.
(6) Dixit, C. K.; Kadimisetty, K.; Otieno, B. A.; Tang, C.; Malla, S.; Krause, C. E.; Rusling, J. F. *Analyst* **2016**, *141*, 536−547.
(7) Mistry, K. K.; Layek, K.; Mahapatra, A.; RoyChaudhuri, C.; Saha, H. *Analyst* **2014**, *139*, 2289−2311.
(8) Wen, W.; Huang, J.; Bao, T.; Zhou, J.; Xia, H.; Zhang, X.; Wang, S.; Zhao, Y. *Biosens. Bioelectron.* **2016**, *83*, 142−148.
(9) (a) Zhu, C.; Yang, G.; Li, H.; Du, D.; Lin, Y. *Anal. Chem.* **2015**, *87*, 230−249. (b) Zeng, Y.; Zhu, Z.; Du, D.; Lin, Y. J. *Electroanal. Chem.* **2016**, DOI: 10.1016/j.jelechem.2016.10.030. (c) Wu, D.; Du, D.; Lin, Y. *TrAC, Trends Anal. Chem.* **2016**, *83*, 95−101. (d) Zhang, W.; Asiri, A. M.; Liu, D.; Du, D.; Lin, Y. *TrAC, Trends Anal. Chem.* **2014**, *54*, 1−10. (e) Zhu, C.; Li, H.; Fu, S.; Du, D.; Lin, Y. *Chem. Soc. Rev.* **2016**, *45*, 517−531.
(10) (a) Chandra, P.; Noh, H. B.; Pallela, R.; Shim, Y. B. *Biosens. Bioelectron.* **2015**, *70*, 418−425. (b) Pallela, R.; Chandra, P.; Noh, H. B.; Shim, Y. B. *Biosens. Bioelectron.* **2016**, *85*, 883−890. (c) Hussain, K. K.; Gurudatt, N. G.; Mir, T. A.; Shim, Y. B. *Biosens. Bioelectron.* **2016**, *83*, 312−318.
(11) Zhu, C.; Du, D.; Lin, Y. *Biosens. Bioelectron.* **2016**, DOI: 10.1016/j.bios.2016.06.045.
(12) (a) Zhu, C.; Du, D.; Lin, Y. *2D Mater.* **2015**, *2*, 032004. (b) Wei, T.; Dai, Z.; Lin, Y.; Du, D. *Electroanalysis* **2016**, *28*, 4−12.
(13) Qin, X.; Xu, A.; Wang, L.; Liu, L.; Chao, L.; He, F.; Tan, Y.; Chen, C.; Xie, Q. *Biosens. Bioelectron.* **2016**, *79*, 914−921.
(14) Singh, V.; Krishnan, S. *Anal. Chem.* **2015**, *87*, 2648−2654.
(15) Jiao, L.; Mu, Z.; Zhu, C.; Wei, Q.; Li, H.; Du, D.; Lin, Y. *Sens. Actuators, B* **2016**, *231*, 513−519.
(16) Li, Q.; Liu, D.; Xu, L.; Xing, R.; Liu, W.; Sheng, K.; Song, H. *ACS Appl. Mater. Interfaces* **2015**, *7*, 22719−22726.
(17) Ali, M. A.; Mondal, K.; Singh, C.; Malhotra, B. D.; Sharma, A. *Nanoscale* **2015**, *7*, 7234−7245.
(18) Wang, N.; Gao, C.; Han, Y.; Huang, X.; Xu, Y.; Cao, X. *J. Mater. Chem. B* **2015**, *3*, 3254−3259.
(19) Su, S.; Zou, M.; Zhao, H.; Yuan, C.; Xu, Y.; Zhang, C.; Wang, L.; Fan, C.; Wang, L. *Nanoscale* **2015**, *7*, 19129−19135.
(20) Zhang, Y.; Li, J.; Wang, Z.; Ma, H.; Wu, D.; Cheng, Q.; Wei, Q. *Sci. Rep.* **2016**, *6*, 23391.
(21) Ji, L.; Yan, T.; Li, Y.; Gao, J.; Wang, Q.; Hu, L.; Wu, D.; Wei, Q.; Du, B. *Sci. Rep.* **2016**, *6*, 21017.
(22) Li, F.; Li, Y.; Dong, Y.; Jiang, L.; Wang, P.; Liu, Q.; Liu, H.; Wei, Q. *Sci. Rep.* **2016**, *6*, 21281.
(23) Wu, D.; Ma, H.; Zhang, Y.; Jia, H.; Yan, T.; Wei, Q. *ACS Appl. Mater. Interfaces* **2015**, *7*, 18786−18793.
(24) Fang, C. S.; Oh, K. H.; Oh, A.; Lee, K.; Park, S.; Kim, S.; Park, J. K.; Yang, H. *Chem. Commun.* **2016**, *52*, 5884−5887.
(25) Shen, W.; Zhuo, Y.; Chai, Y.; Yang, Z.; Han, J.; Yuan, R. *ACS Appl. Mater. Interfaces* **2015**, *7*, 4127−4134.
(26) Lin, Y.; Zhou, Q.; Lin, Y.; Lu, M.; Tang, D. *Anal. Chim. Acta* **2015**, *887*, 67−74.
(27) Vabbina, P. K.; Kaushik, A.; Pokhrel, N.; Bhansali, S.; Pala, N. *Biosens. Bioelectron.* **2015**, *63*, 124−130.
(28) Wang, J.; Wang, X.; Wu, S.; Song, J.; Zhao, Y.; Ge, Y.; Meng, C. *Anal. Chim. Acta* **2016**, *906*, 80−88.
(29) Lin, Y.; Zhou, Q.; Lin, Y.; Tang, D.; Niessner, R.; Knopp, D. *Anal. Chem.* **2015**, *87*, 8531−8540.
(30) Zhai, Q.; Zhang, X.; Li, J.; Wang, E. *Nanoscale* **2016**, *8*, 15303−15308.
(31) Tian, L.; Liu, L.; Li, Y.; Wei, Q.; Cao, W. *Sci. Rep.* **2016**, *6*, 30849.
(32) Zhou, C.; Liu, D.; Xu, L.; Li, Q.; Song, J.; Xu, S.; Xing, R.; Song, H. *Sci. Rep.* **2015**, *5*, 9939.
(33) Qin, X.; Xu, A.; Liu, L.; Deng, W.; Chen, C.; Tan, Y.; Fu, Y.; Xie, Q.; Yao, S. *Chem. Commun.* **2015**, *51*, 8540−8543.
(34) Li, N.; Wang, Y.; Cao, W.; Zhang, Y.; Yan, T.; Du, B.; Wei, Q. *J. Mater. Chem. B* **2015**, *3*, 2006−2011.
(35) Wang, L.; Liu, N.; Ma, Z. *J. Mater. Chem. B* **2015**, *3*, 2867−2872.

DOI: 10.1021/acs.analchem.6b04281
Anal. Chem. 2017, 89, 138−156

(36) Ge, X.; Zhang, A.; Lin, Y.; Du, D. *Biosens. Bioelectron.* **2016**, *80*, 201−207.
(37) Han, J.; Zhuo, Y.; Chai, Y. Q.; Xiang, Y.; Yuan, R. *Anal. Chem.* **2015**, *87*, 1669−1675.
(38) Hong, W.; Lee, S.; Jae Kim, E.; Lee, M.; Cho, Y. *Biosens. Bioelectron.* **2016**, *78*, 181−186.
(39) Ruiz-Valdepenas Montiel, V.; Campuzano, S.; Torrente-Rodriguez, R. M.; Reviejo, A. J.; Pingarron, J. M. *Food Chem.* **2016**, *213*, 595−601.
(40) Zhao, Y.; Zheng, Y.; Kong, R.; Xia, L.; Qu, F. *Biosens. Bioelectron.* **2016**, *75*, 383−388.
(41) Yang, X.; Zhou, X.; Zhang, X.; Qing, Y.; Luo, M.; Liu, X.; Li, C.; Li, Y.; Xia, H.; Qiu, J. *Electroanalysis* **2015**, *27*, 2679−2687.
(42) Diba, F. S.; Kim, S.; Lee, H. J. *Biosens. Bioelectron.* **2015**, *72*, 355−361.
(43) Xu, M.; Wang, R.; Li, Y. *Talanta* **2016**, *148*, 200−208.
(44) Cheng, H.; Xu, L.; Zhang, H.; Yu, A.; Lai, G. *Analyst* **2016**, *141*, 4381−4387.
(45) Gao, J.; Ma, H.; Lv, X.; Yan, T.; Li, N.; Cao, W.; Wei, Q. *Anal. Chim. Acta* **2015**, *893*, 49−56.
(46) Yang, Z.; Jiang, W.; Liu, F.; Zhou, Y.; Yin, H.; Ai, S. *Chem. Commun.* **2015**, *51*, 14671−14673.
(47) Jiaul Haque, A. M.; Kim, J.; Dutta, G.; Kim, S.; Yang, H. *Chem. Commun.* **2015**, *51*, 14493−14496.
(48) Akanda, M. R.; Ju, H. *Anal. Chem.* **2016**, *88*, 9856−9861.
(49) Dutta, G.; Park, S.; Singh, A.; Seo, J.; Kim, S.; Yang, H. *Anal. Chem.* **2015**, *87*, 3574−3578.
(50) Li, F.; Zhang, H.; Wang, Z.; Newbigging, A. M.; Reid, M. S.; Li, X. F.; Le, X. C. *Anal. Chem.* **2015**, *87*, 274−292.
(51) Wang, Q.; Gan, X.; Zang, R.; Chai, Y.; Yuan, Y.; Yuan, R. *Biosens. Bioelectron.* **2016**, *81*, 382−387.
(52) Ren, K.; Wu, J.; Ju, H.; Yan, F. *Anal. Chem.* **2015**, *87*, 1694−1700.
(53) Yang, Z.; Zhuo, Y.; Yuan, R.; Chai, Y. *Anal. Chem.* **2016**, *88*, 5189−5196.
(54) Guo, J.; Wang, J.; Zhao, J.; Guo, Z.; Zhang, Y. *ACS Appl. Mater. Interfaces* **2016**, *8*, 6898−6904.
(55) Wang, Q.; Song, Y.; Xie, H.; Chai, Y.; Yuan, Y.; Yuan, R. *Chem. Commun.* **2015**, *51*, 1255−1258.
(56) Liu, B.; Chen, J.; Wei, Q.; Zhang, B.; Zhang, L.; Tang, D. *Biosens. Bioelectron.* **2015**, *69*, 241−248.
(57) Wang, H.; Li, G.; Zhang, Y.; Zhu, M.; Ma, H.; Du, B.; Wei, Q.; Wan, Y. *Anal. Chem.* **2015**, *87*, 11209−11214.
(58) Zhou, Q.; Li, G.; Zhang, Y.; Zhu, M.; Wan, Y.; Shen, Y. *Anal. Chem.* **2016**, *88*, 9830−9836.
(59) Lin, Y.; Liu, K.; Wang, C.; Li, L.; Liu, Y. *Anal. Chem.* **2015**, *87*, 8047−8051.
(60) Kirschbaum, S. E. K.; Baeumner, A. J. *Anal. Bioanal. Chem.* **2015**, *407*, 3911−3926.
(61) Muzyka, K. *Biosens. Bioelectron.* **2014**, *54*, 393−407.
(62) Habtamu, H. B.; Sentic, M.; Silvestrini, M.; De Leo, L.; Not, T.; Arbault, S.; Manojlovic, D.; Sojic, N.; Ugo, P. *Anal. Chem.* **2015**, *87*, 12080−12087.
(63) Pang, X.; Li, J.; Zhao, Y.; Wu, D.; Zhang, Y.; Du, B.; Ma, H.; Wei, Q. *ACS Appl. Mater. Interfaces* **2015**, *7*, 19260−19267.
(64) Zhang, H.; Han, Z.; Wang, X.; Li, F.; Cui, H.; Yang, D.; Bian, Z. *ACS Appl. Mater. Interfaces* **2015**, *7*, 7599−7604.
(65) Zhou, L.; Huang, J.; Yu, B.; You, T. *Sci. Rep.* **2016**, *6*, 22234.
(66) Zhu, W.; Lv, X.; Wang, Q.; Ma, H.; Wu, D.; Yan, T.; Hu, L.; Du, B.; Wei, Q. *Sci. Rep.* **2016**, *6*, 20348.
(67) Ma, H.; Li, X.; Yan, T.; Li, Y.; Zhang, Y.; Wu, D.; Wei, Q.; Du, B. *Biosens. Bioelectron.* **2016**, *79*, 379−385.
(68) Wu, D.; Liu, Y.; Wang, Y.; Hu, L.; Ma, H.; Wang, G.; Wei, Q. *Sci. Rep.* **2016**, *6*, 20511.
(69) Zhang, X.; Tan, X.; Zhang, B.; Miao, W.; Zou, G. *Anal. Chem.* **2016**, *88*, 6947−6953.
(70) Wang, H.; Yuan, Y.; Zhuo, Y.; Chai, Y.; Yuan, R. *Anal. Chem.* **2016**, *88*, 2258−2265.
(71) Wang, J.; Zhuo, Y.; Zhou, Y.; Wang, H.; Yuan, R.; Chai, Y. *ACS Appl. Mater. Interfaces* **2016**, *8*, 12968−12975.
(72) Chou, H.-T.; Fu, C.-Y.; Lee, C.-Y.; Tai, N.-H.; Chang, H. Y. *Biosens. Bioelectron.* **2015**, *71*, 476−482.
(73) Wang, J. X.; Zhuo, Y.; Zhou, Y.; Yuan, R.; Chai, Y. Q. *Biosens. Bioelectron.* **2015**, *71*, 407−413.
(74) Zhou, L.; Huang, J.; Yu, B.; Liu, Y.; You, T. *ACS Appl. Mater. Interfaces* **2015**, *7*, 24438−24445.
(75) Liu, J.; Cui, M.; Zhou, H.; Zhang, S. *Sci. Rep.* **2016**, *6*, 30577.
(76) Wang, H.; Yuan, Y.; Chai, Y.; Yuan, R. *Biosens. Bioelectron.* **2015**, *68*, 72−77.
(77) Zhang, L.; He, Y.; Wang, H.; Yuan, Y.; Yuan, R.; Chai, Y. *Biosens. Bioelectron.* **2015**, *74*, 924−930.
(78) Liu, Y.; Wang, H.; Xiong, C.; Chai, Y.; Yuan, R. *Biosens. Bioelectron.* **2017**, *87*, 779−785.
(79) Liu, Y.; Zhang, Q.; Wang, H.; Yuan, Y.; Chai, Y.; Yuan, R. *Biosens. Bioelectron.* **2015**, *71*, 164−170.
(80) Liang, W. B.; Yang, M. Z.; Zhuo, Y.; Zheng, Y. N.; Xiong, C. Y.; Chai, Y. Q.; Yuan, R. *Chem. Sci.* **2016**, DOI: 10.1039/C6SC02801B.
(81) Liang, W.; Fan, C.; Zhuo, Y.; Zheng, Y.; Xiong, C.; Chai, Y.; Yuan, R. *Anal. Chem.* **2016**, *88*, 4940−4948.
(82) Chen, A.; Gui, G. F.; Zhuo, Y.; Chai, Y. Q.; Xiang, Y.; Yuan, R. *Anal. Chem.* **2015**, *87*, 6328−6334.
(83) Huang, T.; Meng, Q.; Jie, G. *Biosens. Bioelectron.* **2015**, *66*, 84−88.
(84) Meng, H. M.; Zhang, X.; Lv, Y.; Zhao, Z.; Wang, N. N.; Fu, T.; Fan, H.; Liang, H.; Qiu, L.; Zhu, G.; Tan, W. *ACS Nano* **2014**, *8*, 6171−6181.
(85) Wang, H.; Yuan, Y.; Zhuo, Y.; Chai, Y.; Yuan, R. *Anal. Chem.* **2016**, *88*, 5797−5803.
(86) Liu, X.; Xu, Y.; Wan, D. B.; Xiong, Y. H.; He, Z. Y.; Wang, X. X.; Gee, S. J.; Ryu, D. J.; Hammock, B. D. *Anal. Chem.* **2015**, *87*, 1387−1394.
(87) Rossotti, M. A.; Pirez, M.; Gonzalez-Techera, A.; Cui, Y. L.; Bever, C. S.; Lee, K. S. S.; Morisseau, C.; Leizagoyen, C.; Gee, S.; Hammock, B. D.; Gonzalez-Sapienza, G. *Anal. Chem.* **2015**, *87*, 11907−11914.
(88) Li, H.; Sun, Y.; Elseviers, J.; Muyldermans, S.; Liu, S.; Wan, Y. *Analyst* **2014**, *139*, 3718−3721.
(89) Mu, X.; Tong, Z.; Huang, Q.; Liu, B.; Liu, Z.; Hao, L.; Dong, H.; Zhang, J.; Gao, C. *Sensors* **2016**, *16*, 308.
(90) Zhao, W. W.; Xu, J. J.; Chen, H. Y. *Chem. Soc. Rev.* **2015**, *44*, 729−741.
(91) Zhou, H.; Liu, J.; Zhang, S. *TrAC, Trends Anal. Chem.* **2015**, *67*, 56−73.
(92) Pang, X.; Zhang, Y.; Liu, C.; Huang, Y.; Wang, Y.; Pan, J.; Wei, Q.; Du, B. *J. Mater. Chem. B* **2016**, *4*, 4612−4619.
(93) Li, Y.; Dai, H.; Zhang, Q.; Zhang, S.; Chen, S.; Hong, Z.; Lin, Y. *J. Mater. Chem. B* **2016**, *4*, 2591−2597.
(94) Wang, H.; Wang, Y.; Zhang, Y.; Wang, Q.; Ren, X.; Wu, D.; Wei, Q. *Sci. Rep.* **2016**, *6*, 27385.
(95) Lin, Y.; Zhou, Q.; Tang, D.; Niessner, R.; Yang, H.; Knopp, D. *Anal. Chem.* **2016**, *88*, 7858−7866.
(96) Song, J.; Wang, J.; Wang, X.; Zhao, W.; Zhao, Y.; Wu, S.; Gao, Z.; Yuan, J.; Meng, C. *Biosens. Bioelectron.* **2016**, *80*, 614−620.
(97) Yang, H.; Sun, G.; Zhang, L.; Zhang, Y.; Song, X.; Yu, J.; Ge, S. *Sens. Actuators, B* **2016**, *234*, 658−666.
(98) Zhu, H.; Fan, G. C.; Abdel-Halim, E. S.; Zhang, J. R.; Zhu, J. J. *Biosens. Bioelectron.* **2016**, *77*, 339−346.
(99) Dai, H.; Gong, L.; Zhang, S.; Xu, G.; Li, Y.; Hong, Z.; Lin, Y. *Biosens. Bioelectron.* **2016**, *77*, 928−935.
(100) Zhang, Y.; Shoaib, A.; Li, J.; Ji, M.; Liu, J.; Xu, M.; Tong, B.; Zhang, J.; Wei, Q. *Biosens. Bioelectron.* **2016**, *79*, 866−873.
(101) Yu, X.; Wang, Y.; Chen, X.; Wu, K.; Chen, D.; Ma, M.; Huang, Z.; Wu, W.; Li, C. *Anal. Chem.* **2015**, *87*, 4237−4244.
(102) Fan, G. C.; Zhu, H.; Du, D.; Zhang, J. R.; Zhu, J. J.; Lin, Y. *Anal. Chem.* **2016**, *88*, 3392−3399.
(103) Gong, L.; Dai, H.; Zhang, S.; Lin, Y. *Anal. Chem.* **2016**, *88*, 5775−5782.

DOI: 10.1021/acs.analchem.6b04281
Anal. Chem. 2017, 89, 138−156

(104) Dai, H.; Zhang, S.; Hong, Z.; Lin, Y. *Anal. Chem.* **2016**, *88*, 9532−9538.
(105) Barroso, J.; Saa, L.; Grinyte, R.; Pavlov, V. *Biosens. Bioelectron.* **2016**, *77*, 323−329.
(106) Zhu, Y. C.; Zhang, N.; Ruan, Y. F.; Zhao, W. W.; Xu, J. J.; Chen, H. Y. *Anal. Chem.* **2016**, *88*, 5626−5630.
(107) Zhang, N.; Ma, Z. Y.; Ruan, Y. F.; Zhao, W. W.; Xu, J. J.; Chen, H. Y. *Anal. Chem.* **2016**, *88*, 1990−1994.
(108) Shu, J.; Qiu, Z.; Zhuang, J.; Xu, M.; Tang, D. *ACS Appl. Mater. Interfaces* **2015**, *7*, 23812−23818.
(109) Ma, Z. Y.; Ruan, Y. F.; Xu, F.; Zhao, W. W.; Xu, J. J.; Chen, H. Y. *Anal. Chem.* **2016**, *88*, 3864−3871.
(110) Zhuang, J.; Tang, D.; Lai, W.; Xu, M.; Tang, D. *Anal. Chem.* **2015**, *87*, 9473−9480.
(111) Wen, G.; Ju, H. *Anal. Chem.* **2016**, *88*, 8339−8345.
(112) Zhao, W. W.; Han, Y. M.; Zhu, Y. C.; Zhang, N.; Xu, J. J.; Chen, H. Y. *Anal. Chem.* **2015**, *87*, 5496−5499.
(113) Zhang, Y.; Sun, G.; Yang, H.; Yu, J.; Yan, M.; Song, X. *Biosens. Bioelectron.* **2016**, *79*, 55−62.
(114) Ge, S.; Liang, L.; Lan, F.; Zhang, Y.; Wang, Y.; Yan, M.; Yu, J. *Sens. Actuators, B* **2016**, *234*, 324−331.
(115) Shu, J.; Qiu, Z.; Zhou, Q.; Lin, Y.; Lu, M.; Tang, D. *Anal. Chem.* **2016**, *88*, 2958−2966.
(116) Li, H.; Mu, Y.; Yan, J.; Cui, D.; Ou, W.; Wan, Y.; Liu, S. *Anal. Chem.* **2015**, *87*, 2007−2015.
(117) Kim, K. S.; Jang, J. R.; Choe, W. S.; Yoo, P. J. *Biosens. Bioelectron.* **2015**, *71*, 214−221.
(118) Li, Z.; Ye, Z.; Fu, Y.; Xiong, Y.; Li, Y. *Anal. Methods* **2016**, *8*, 548−553.
(119) Sonuc Karaboga, M. N.; Simsek, C. S.; Sezginturk, M. K. *Biosens. Bioelectron.* **2016**, *84*, 22−29.
(120) Chuang, C. H.; Du, Y. C.; Wu, T. F.; Chen, C. H.; Lee, D. H.; Chen, S. M.; Huang, T. C.; Wu, H. P.; Shaikh, M. O. *Biosens. Bioelectron.* **2016**, *84*, 126−132.
(121) Kim, J.; Cho, H.; Han, S. I.; Han, K. H. *Anal. Chem.* **2016**, *88*, 4857−4863.
(122) Krithiga, N.; Viswanath, K. B.; Vasantha, V. S.; Jayachitra, A. *Biosens. Bioelectron.* **2016**, *79*, 121−129.
(123) Pal, N.; Sharma, S.; Gupta, S. *Biosens. Bioelectron.* **2016**, *77*, 270−276.
(124) Bedatty Fernandes, F. C.; Patil, A. V.; Bueno, P. R.; Davis, J. J. *Anal. Chem.* **2015**, *87*, 12137−12144.
(125) Malvano, F.; Albanese, D.; Pilloton, R.; Di Matteo, M. *Food Chem.* **2016**, *212*, 688−694.
(126) Sayikli Simsek, C.; Nur Sonuc Karaboga, M.; Sezginturk, M. K. *Talanta* **2015**, *144*, 210−218.
(127) Mehta, J.; Vinayak, P.; Tuteja, S. K.; Chhabra, V. A.; Bhardwaj, N.; Paul, A. K.; Kim, K. H.; Deep, A. *Biosens. Bioelectron.* **2016**, *83*, 339−346.
(128) Shi, Z.; Tian, Y.; Wu, X.; Li, C.; Yu, L. *Anal. Methods* **2015**, *7*, 4957−4964.
(129) Li, G.; Zhu, M.; Ma, L.; Yan, J.; Lu, X.; Shen, Y.; Wan, Y. *ACS Appl. Mater. Interfaces* **2016**, *8*, 13830−13839.
(130) Bhardwaj, S. K.; Bhardwaj, N.; Mohanta, G. C.; Kumar, P.; Sharma, A. L.; Kim, K. H.; Deep, A. *ACS Appl. Mater. Interfaces* **2015**, *7*, 26124−26130.
(131) Balakrishnan, S. R.; Hashim, U.; Gopinath, S. C.; Poopalan, P.; Ramayya, H. R.; Veeradasan, P.; Haarindraprasad, R.; Ruslinda, A. R. *Biosens. Bioelectron.* **2016**, *84*, 44−52.
(132) Selvam, A. P.; Muthukumar, S.; Kamakoti, V.; Prasad, S. *Sci. Rep.* **2016**, *6*, 23111.
(133) Kaur, G.; Tomar, M.; Gupta, V. *Biosens. Bioelectron.* **2016**, *80*, 294−299.
(134) Soares, J. C.; Shimizu, F. M.; Soares, A. C.; Caseli, L.; Ferreira, J.; Oliveira, O. N., Jr. *ACS Appl. Mater. Interfaces* **2015**, *7*, 11833−11841.
(135) Eissa, S.; Jimenez, G. C.; Mahvash, F.; Guermoune, A.; Tlili, C.; Szkopek, T.; Zourob, M.; Siaj, M. *Nano Res.* **2015**, *8*, 1698−1709.
(136) Xu, T. S. *Biochem. Eng. J.* **2016**, *105*, 36−43.
(137) Ali, M. A.; Solanki, P. R.; Srivastava, S.; Singh, S.; Agrawal, V. V.; John, R.; Malhotra, B. D. *ACS Appl. Mater. Interfaces* **2015**, *7*, 5837−5846.
(138) Johari-Ahar, M.; Rashidi, M. R.; Barar, J.; Aghaie, M.; Mohammadnejad, D.; Ramazani, A.; Karami, P.; Coukos, G.; Omidi, Y. *Nanoscale* **2015**, *7*, 3768−3779.
(139) Patil, A. V.; Bedatty Fernandes, F. C.; Bueno, P. R.; Davis, J. J. *Anal. Chem.* **2015**, *87*, 944−950.
(140) Liu, W.; Tian, C.; Yan, M.; Zhao, L.; Ma, C.; Li, T.; Xu, J.; Wang, J. *Lab Chip* **2016**, *16*, 4106−4120.
(141) Yang, H.; Zhou, H.; Hao, H.; Gong, Q.; Nie, K. *Sens. Actuators, B* **2016**, *229*, 297−304.
(142) Jarocka, U.; Sawicka, R.; Góra-Sochacka, A.; Sirko, A.; Dehaen, W.; Radecki, J.; Radecka, H. *Sens. Actuators, B* **2016**, *228*, 25−30.
(143) Anik, U.; Tepeli, Y.; Diouani, M. F. *Anal. Chem.* **2016**, *88*, 6151−6153.
(144) Wan, J.; Ai, J.; Zhang, Y.; Geng, X.; Gao, Q.; Cheng, Z. *Sci. Rep.* **2016**, *6*, 19806.
(145) Marcali, M.; Elbuken, C. *Lab Chip* **2016**, *16*, 2494−2503.
(146) Hatsuki, R.; Honda, A.; Kajitani, M.; Yamamoto, T. *Front. Microbiol.* **2015**, *6*, 940.
(147) Casalini, S.; Dumitru, A. C.; Leonardi, F.; Bortolotti, C. A.; Herruzo, E. T.; Campana, A.; de Oliveira, R. F.; Cramer, T.; Garcia, R.; Biscarini, F. *ACS Nano* **2015**, *9*, 5051−5062.
(148) Tran, T. T.; Mulchandani, A. *TrAC, Trends Anal. Chem.* **2016**, *79*, 222−232.
(149) Aroonyadet, N.; Wang, X.; Song, Y.; Chen, H.; Cote, R. J.; Thompson, M. E.; Datar, R. H.; Zhou, C. *Nano Lett.* **2015**, *15*, 1943−1951.
(150) Lee, I. K.; Jeun, M.; Jang, H. J.; Cho, W. J.; Lee, K. H. *Nanoscale* **2015**, *7*, 16789−16797.
(151) Zhang, C.; Xu, J. Q.; Li, Y. T.; Huang, L.; Pang, D. W.; Ning, Y.; Huang, W. H.; Zhang, Z. Y.; Zhang, G. J. *Anal. Chem.* **2016**, *88*, 4048−4054.
(152) Vardi, Y.; Cohen-Hoshen, E.; Shalem, G.; Bar-Joseph, I. *Nano Lett.* **2016**, *16*, 748−752.
(153) Richner, P.; Kress, S. J. P.; Norris, D. J.; Poulikakos, D. *Nanoscale* **2016**, *8*, 6028−6034.
(154) Vaidyanathan, R.; Rauf, S.; Grewal, Y. S.; Spadafora, L. J.; Shiddiky, M. J.; Cangelosi, G. A.; Trau, M. *Anal. Chem.* **2015**, *87*, 11673−11681.
(155) Han, D.; Park, J. K. *Lab Chip* **2016**, *16*, 1189−1196.
(156) Yin, T.; Qin, W. *TrAC, Trends Anal. Chem.* **2013**, *51*, 79−86.
(157) Zhang, Q.; Prabhu, A.; San, A.; Al-Sharab, J. F.; Levon, K. *Biosens. Bioelectron.* **2015**, *72*, 100−106.
(158) Figueiredo, A.; Vieira, N. C.; dos Santos, J. F.; Janegitz, B. C.; Aoki, S. M.; Junior, P. P.; Lovato, R. L.; Nogueira, M. L.; Zucolotto, V.; Guimaraes, F. E. *Sci. Rep.* **2015**, *5*, 7865.
(159) Arif, S.; Qudsia, S.; Urooj, S.; Chaudry, N.; Arshad, A.; Andleeb, S. *Biosens. Bioelectron.* **2015**, *65*, 62−70.
(160) Luo, Y.; Liu, T.; Zhu, J.; Kong, L.; Wang, W.; Tan, L. *Anal. Chem.* **2015**, *87*, 11277−11284.
(161) Deng, X.; Chen, M.; Fu, Q.; Smeets, N. M.; Xu, F.; Zhang, Z.; Filipe, C. D.; Hoare, T. *ACS Appl. Mater. Interfaces* **2016**, *8*, 1893−1902.
(162) March, C.; Garcia, J. V.; Sanchez, A.; Arnau, A.; Jimenez, Y.; Garcia, P.; Manclus, J. J.; Montoya, A. *Biosens. Bioelectron.* **2015**, *65*, 1−8.
(163) Tiwari, J. N.; Vij, V.; Kemp, K. C.; Kim, K. S. *ACS Nano* **2016**, *10*, 46−80.
(164) Giri, B.; Pandey, B.; Neupane, B.; Ligler, F. S. *TrAC, Trends Anal. Chem.* **2016**, *79*, 326−334.
(165) Wang, C. C.; Hennek, J. W.; Ainla, A.; Kumar, A. A.; Lan, W. J.; Im, J.; Smith, B. S.; Zhao, M. X.; Whitesides, G. M. *Anal. Chem.* **2016**, *88*, 6326−6333.
(166) Lin, X.; Sun, X.; Luo, S.; Liu, B.; Yang, C. *TrAC, Trends Anal. Chem.* **2016**, *80*, 132−148.
(167) Xia, Y.; Si, J.; Li, Z. *Biosens. Bioelectron.* **2016**, *77*, 774−789.

DOI: 10.1021/acs.analchem.6b04281
Anal. Chem. 2017, 89, 138−156

(168) Arduini, F.; Micheli, L.; Moscone, D.; Palleschi, G.; Piermarini, S.; Ricci, F.; Volpe, G. *TrAC, Trends Anal. Chem.* **2016**, *79*, 114−126.
(169) Samiei, E.; Tabrizian, M.; Hoorfar, M. *Lab Chip* **2016**, *16*, 2376−2396.
(170) Li, X.; Liu, X. Y. *Adv. Healthcare Mater.* **2016**, *5*, 1326−1335.
(171) Sun, G.; Zhang, L.; Zhang, Y.; Yang, H.; Ma, C.; Ge, S.; Yan, M.; Yu, J.; Song, X. *Biosens. Bioelectron.* **2015**, *71*, 30−36.
(172) Hou, C.; Fan, S.; Lang, Q.; Liu, A. *Anal. Chem.* **2015**, *87*, 3382−3387.
(173) Li, S.; Wang, Y.; Ge, S.; Yu, J.; Yan, M. *Biosens. Bioelectron.* **2015**, *71*, 18−24.
(174) Wu, K.; Zhang, Y.; Wang, Y.; Ge, S.; Yan, M.; Yu, J.; Song, X. *ACS Appl. Mater. Interfaces* **2015**, *7*, 24330−24337.
(175) Yang, L.; Tao, Y.; Yue, G.; Li, R.; Qiu, B.; Guo, L.; Lin, Z.; Yang, H. *Anal. Chem.* **2016**, *88*, 5097−5103.
(176) Chen, A.; Ma, S.; Zhuo, Y.; Chai, Y.; Yuan, R. *Anal. Chem.* **2016**, *88*, 3203−3210.
(177) Zhang, P.; Wu, X.; Yuan, R.; Chai, Y. *Anal. Chem.* **2015**, *87*, 3202−3207.
(178) Wu, L.; Ma, C.; Zheng, X.; Liu, H.; Yu, J. *Biosens. Bioelectron.* **2015**, *68*, 413−420.
(179) Shin, S.; Zhang, Y. S.; Kim, D.; Manbohi, A.; Avci, H.; Silvestri, A.; Aleman, J.; Hu, N.; Kilic, T.; Keung, W.; Righi, M.; Assawes, P.; Alhadrami, H. A.; Li, R. A.; Dokmeci, M. R.; Khademhosseini, A. *Anal. Chem.* **2016**, *88*, 10019−10027.
(180) Riahi, R.; Shaegh, S. A. M.; Ghaderi, M.; Zhang, Y. S.; Shin, S. R.; Aleman, J.; Massa, S.; Kim, D.; Dokmeci, M. R.; Khademhosseini, A. *Sci. Rep.* **2016**, *6*, 24598.
(181) Santos, I. C.; Mesquita, R. B. R.; Rangel, A. S. S. *Anal. Chim. Acta* **2015**, *891*, 171−178.
(182) Shao, G.; Lu, D.; Fu, Z.; Du, D.; Ozanich, R. M.; Wang, W.; Lin, Y. *Analyst* **2016**, *141*, 206−215.
(183) Huang, J. M. Y.; Henihan, G.; Macdonald, D.; Michalowski, A.; Templeton, K.; Gibb, A. P.; Schulze, H.; Bachmann, T. T. *Anal. Chem.* **2015**, *87*, 7738−7745.
(184) Cortina, M. E.; Melli, L. J.; Roberti, M.; Mass, M.; Longinotti, G.; Tropea, S.; Lloret, P.; Serantes, D. A. R.; Salomon, F.; Lloret, M.; Caillava, A. J.; Restuccia, S.; Altcheh, J.; Buscaglia, C. A.; Malatto, L.; Ugalde, J. E.; Fraigi, L.; Moina, C.; Ybarra, G.; Ciocchini, A. E.; Comerci, D. J. *Biosens. Bioelectron.* **2016**, *80*, 24−33.
(185) Sun, G.; Yang, H.; Zhang, Y.; Yu, J.; Ge, S.; Yan, M.; Song, X. *Biosens. Bioelectron.* **2015**, *74*, 823−829.
(186) Munge, B. S.; Stracensky, T.; Gamez, K.; DiBiase, D.; Rusling, J. F. *Electroanalysis* **2016**, DOI: 10.1002/elan.201600183.
(187) Chiriacò, M. S.; Primiceri, E.; De Feo, F.; Montanaro, A.; Monteduro, A. G.; Tinelli, A.; Megha, M.; Carati, D.; Maruccio, G. *Biosens. Bioelectron.* **2016**, *79*, 9−14.
(188) Otieno, B. A.; Krause, C. E.; Jones, A. L.; Kremer, R. B.; Rusling, J. F. *Anal. Chem.* **2016**, *88*, 9269−9275.
(189) Liu, H.; Liu, W.; Yang, X.; Zhou, X.; Xing, D. *Anal. Chem.* **2016**, *88*, 10191−10197.
(190) Wu, M. S.; Liu, Z.; Shi, H. W.; Chen, H. Y.; Xu, J. J. *Anal. Chem.* **2015**, *87*, 530−537.
(191) Zhai, Q.; Zhang, X.; Han, Y.; Zhai, J.; Li, J.; Wang, E. *Anal. Chem.* **2016**, *88*, 945−951.
(192) Shi, H. W.; Zhao, W.; Liu, Z.; Liu, X. C.; Xu, J. J.; Chen, H. Y. *Anal. Chem.* **2016**, *88*, 8795−8801.
(193) Kadimisetty, K.; Malla, S.; Sardesai, N. P.; Joshi, A. A.; Faria, R. C.; Lee, N. H.; Rusling, J. F. *Anal. Chem.* **2015**, *87*, 4472−4478.
(194) Robinson, J. T.; Jorgolli, M.; Shalek, A. K.; Yoon, M. H.; Gertner, R. S.; Park, H. *Nat. Nanotechnol.* **2012**, *7*, 180−184.
(195) Dabkowska, A. P.; Niman, C. S.; Piret, G.; Persson, H.; Wacklin, H. P.; Linke, H.; Prinz, C. N.; Nylander, T. *Nano Lett.* **2014**, *14*, 4286−4292.
(196) Nasr, B.; Chana, G.; Lee, T. T.; Nguyen, T.; Abeyrathne, C.; D'Abaco, G. M.; Dottori, M.; Skafidas, E. *Small* **2015**, *11*, 2862−2868.
(197) Bishop, G. W.; Satterwhite-Warden, J. E.; Kadimisetty, K.; Rusling, J. F. *Nanotechnology* **2016**, *27*, 284002.
(198) Yang, H.; Rahman, M. T.; Du, D.; Panat, R.; Lin, Y. *Sens. Actuators, B* **2016**, *230*, 600−606.
(199) Gross, B. C.; Erkal, J. L.; Lockwood, S. Y.; Chen, C. P.; Spence, D. M. *Anal. Chem.* **2014**, *86*, 3240−3253.
(200) Kadimisetty, K.; Mosa, I. M.; Malla, S.; Satterwhite-Warden, J. E.; Kuhns, T. M.; Faria, R. C.; Lee, N. H.; Rusling, J. F. *Biosens. Bioelectron.* **2016**, *77*, 188−193.
(201) Tian, T.; Li, J.; Song, Y.; Zhou, L.; Zhu, Z.; Yang, C. J. *Lab Chip* **2016**, *16*, 1139−1151.
(202) Zhang, J.; Xiang, Y.; Wang, M.; Basu, A.; Lu, Y. *Angew. Chem., Int. Ed.* **2016**, *55*, 732−736.
(203) Lan, T.; Zhang, J.; Lu, Y. *Biotechnol. Adv.* **2016**, *34*, 331−341.
(204) Xie, S.; Yuan, Y.; Song, Y.; Zhuo, Y.; Li, T.; Chai, Y.; Yuan, R. *Chem. Commun.* **2014**, *50*, 15932−15935.
(205) Zhang, D.; Liu, Q. *Biosens. Bioelectron.* **2016**, *75*, 273−284.
(206) Arts, R.; den Hartog, I.; Zijlema, S. E.; Thijssen, V.; van der Beelen, S. H. E.; Merkx, M. *Anal. Chem.* **2016**, *88*, 4525−4532.
(207) Kwon, D.; Joo, J.; Lee, S.; Jeon, S. *Anal. Chem.* **2013**, *85*, 12134−12137.
(208) (a) Ye, R.; Zhu, C.; Song, Y.; Lu, Q.; Ge, X.; Yang, X.; Zhu, M.; Du, D.; Li, H.; Lin, Y. *Small* **2016**, *12*, 3094−3100. (b) Ye, R.; Zhu, C.; Song, Y.; Song, J.; Fu, S.; Lu, Q.; Yang, X.; Zhu, M.; Du, D.; Li, H.; Lin, Y. *Nanoscale* **2016**, DOI: 10.1039/C6NR06870G.
(209) Zhang, Y.; Yang, J.; Nie, J.; Yang, J.; Gao, D.; Zhang, L.; Li, J. *Chem. Commun.* **2016**, *52*, 3474−3477.
(210) Yan, L.; Zhu, Z.; Zou, Y.; Huang, Y. S.; Liu, D. W.; Jia, S. S.; Xu, D. M.; Wu, M.; Zhou, Y.; Zhou, S.; Yang, C. J. *J. Am. Chem. Soc.* **2013**, *135*, 3748−3751.
(211) Xiang, Y.; Lu, Y. *Nat. Chem.* **2011**, *3*, 697−703.
(212) Lin, B. Q.; Liu, D.; Yan, J. M.; Qiao, Z.; Zhong, Y. X.; Yan, J. W.; Zhu, Z.; Ji, T. H.; Yang, C. J. *ACS Appl. Mater. Interfaces* **2016**, *8*, 6890−6897.
(213) Xiang, Y.; Lu, Y. *Anal. Chem.* **2012**, *84*, 4174−4178.
(214) Tang, D.; Lin, Y.; Zhou, Q.; Lin, Y.; Li, P.; Niessner, R.; Knopp, D. *Anal. Chem.* **2014**, *86*, 11451−11458.
(215) Gao, Z.; Tang, D.; Xu, M.; Chen, G.; Yang, H. *Chem. Commun.* **2014**, *50*, 6256−6258.
(216) Liu, X.; Situ, A.; Kang, Y.; Villabroza, K. R.; Liao, Y.; Chang, C. H.; Donahue, T.; Nel, A. E.; Meng, H. *ACS Nano* **2016**, *10*, 2702−2715.
(217) Jiang, L.; Li, L.; He, X. D.; Yi, Q. Y.; He, B.; Cao, J.; Pan, W.; Gu, Z. *Biomaterials* **2015**, *52*, 126−139.
(218) Zhao, Y.; Du, D.; Lin, Y. *Biosens. Bioelectron.* **2015**, *72*, 348−354.
(219) Wang, Q.; Liu, F.; Yang, X.; Wang, K.; Wang, H.; Deng, X. *Biosens. Bioelectron.* **2015**, *64*, 161−164.
(220) Zhu, Z.; Guan, Z.; Liu, D.; Jia, S.; Li, J.; Lei, Z.; Lin, S.; Ji, T.; Tian, Z.; Yang, C. J. *Angew. Chem., Int. Ed.* **2015**, *54*, 10448−10453.
(221) Ji, T.; Liu, D.; Liu, F.; Li, J.; Ruan, Q.; Song, Y.; Tian, T.; Zhu, Z.; Zhou, L. J.; Lin, H.; Yang, C.; Wang, D. *Chem. Commun.* **2016**, *52*, 8452−8454.
(222) Tang, D.; Zhang, B.; Liu, B.; Chen, G.; Lu, M. *Biosens. Bioelectron.* **2014**, *55*, 255−258.
(223) Shu, J.; Qiu, Z.; Zhou, Q.; Lin, Y.; Lu, M.; Tang, D. *Anal. Chem.* **2016**, *88*, 2958−2966.
(224) Roda, A.; Michelini, E.; Zangheri, M.; Di Fusco, M.; Calabria, D.; Simoni, P. *TrAC, Trends Anal. Chem.* **2016**, *79*, 317−325.
(225) Wei, Q. S.; Nagi, R.; Sadeghi, K.; Feng, S.; Yan, E.; Ki, S. J.; Caire, R.; Tseng, D.; Ozcan, A. *ACS Nano* **2014**, *8*, 1121−1129.
(226) Rodriguez-Manzano, J.; Karymov, M. A.; Begolo, S.; Selck, D. A.; Zhukov, D. V.; Jue, E.; Ismagilov, R. F. *ACS Nano* **2016**, *10*, 3102−3113.
(227) Vashist, S. K.; van Oordt, T.; Schneider, E. M.; Zengerle, R.; von Stetten, F.; Luong, J. H. T. *Biosens. Bioelectron.* **2015**, *67*, 248−255.
(228) Khan, S. A.; Smith, G. T.; Seo, F.; Ellerbee, A. K. *Biosens. Bioelectron.* **2015**, *64*, 30−35.
(229) Wang, L.-J.; Chang, Y.-C.; Ge, X.; Osmanson, A. T.; Du, D.; Lin, Y.; Li, L. *ACS Sens.* **2016**, *1*, 366−373.

DOI: 10.1021/acs.analchem.6b04281
Anal. Chem. 2017, 89, 138−156

(230) Berg, B.; Cortazar, B.; Tseng, D.; Ozkan, H.; Feng, S.; Wei, Q. S.; Chan, R. Y. L.; Burbano, J.; Farooqui, Q.; Lewinski, M.; Di Carlo, D.; Garner, O. B.; Ozcan, A. *ACS Nano* **2015**, *9*, 7857−7866.
(231) Nemiroski, A.; Christodouleas, D. C.; Hennek, J. W.; Kumar, A. A.; Maxwell, E. J.; Fernandez-Abedul, M. T.; Whitesides, G. M. *Proc. Natl. Acad. Sci. U. S. A.* **2014**, *111*, 11984−11989.
(232) Aronoff-Spencer, E.; Venkatesh, A. G.; Sun, A.; Brickner, H.; Looney, D.; Hall, D. A. *Biosens. Bioelectron.* **2016**, *86*, 690−696.
(233) Dou, Y.; Jiang, Z.; Deng, W.; Su, J.; Chen, S.; Song, H.; Aldalbahi, A.; Zuo, X.; Song, S.; Shi, J.; Fan, C. *J. Electroanal. Chem.* **2016**, DOI: 10.1016/j.jelechem.2016.04.022.

DOI: 10.1021/acs.analchem.6b04281
Anal. Chem. 2017, 89, 138−156